DISCUSSION

LD mapping of 1q21–23 in Japanese subjects identified multiple LD blocks in the region, and one block containing *FCRL3* was associated with rheumatoid arthritis. This association was replicated in a second Japanese case-control set. The rheumatoid arthritis–associated allele was also associated with increased risk of other autoimmune disorders, such as AITD (Graves' disease and Hashimoto's thyroiditis) and SLE. Recent reports on autoimmune disease–associated polymorphisms show that some disease-susceptible variants are limited to specific ethnic groups[12] whereas others are widely dispersed but significantly associated with disease in only specific ethnic groups[41,42]. We evaluated four-SNP haplotypes in *FCRL3* in African American, European American and Asian (Korean and Japanese) subjects and found weaker LD in African Americans than in other groups and substantial differences in allelic frequency among the groups (**Supplementary Table 3** online).

Although the evidence presented here for *FCRL3* being an autoimmune disease–susceptibility gene is powerful, additional autoimmune disease–related genes probably exist in this region. For example, 1q23 is a good candidate locus for SLE susceptibility[6], particularly involving the association of the classical FcγR genes with SLE susceptibility in the Japanese population[19], although those variants are not in LD with SNP −169C→T in our Japanese subjects ($\Delta < 0.05$, **Fig. 1a**). Multiple SLE susceptibility genes are also homologous to human 1q23 in mouse models of SLE[43].

Further evaluation of polymorphism associations showed that a SNP in the promoter region of *FCRL3* alters expression of *FCRL3* through NF-κB binding. Because higher expression of *FCRL3* was observed in individuals with susceptible alleles, and augmented autoantibody production was associated with the susceptible genotype, important steps in the sequence of events leading to autoimmunity must proceed through *FCRL3*. That the susceptible allele is associated with *HLA-DRB1* in rheumatoid arthritis is consistent with *FCRL3* functioning in the context of HLA class II restriction, which is usually seen in the interaction between T cells and antigen-presenting cells, including B cells. Moreover, together with the dominant expression of *FCRL3* on B cells and the importance of B cells suggested by a recent clinical trial of B cell–depleting therapy[44], the present findings might provide a genetic basis for B-cell abnormality in autoimmunity.

Although the precise function of *FCRL3* is unknown, its predicted molecular structure suggests that it is a membranous protein that conveys signals into cells through a cytoplasmic domain containing an immunoreceptor-tyrosine activation motif and an immunoreceptor-tyrosine inhibitory motif[14]. An *in vitro* study showing the binding of tyrosine kinases syk and ZAP70 to the immunoreceptor-tyrosine activation motif region and of tyrosine phosphatases SHP-1 and SHP-2 to the immunoreceptor-tyrosine inhibitory motif region[17] supports the proposed signaling function of *FCRL3*. In a previous study examining *in situ* hybridization in human tonsil, *FCRL3* was expressed in the germinal center, with particularly high expression in the light zone[16], suggesting that *FCRL3* functions predominantly in centrocytes. The present finding that CD40 stimulation, which is important in germinal-center formation[45], upregulates *FCRL3* expression in B cells could indicate that *FCRL3* is specifically expressed in germinal-center centrocytes under the influence of CD40 signals. In the light zone, centrocytes undergo clonal selection and affinity maturation regulated by positive and negative signals from antigen receptors and coreceptors[46]. High expression of *FCRL3* and augmented autoantibody production in individuals with the disease-susceptible genotype is consistent with the idea that *FCRL3* influences the fate of B cells and augments the emergence of self-reactive cells in the germinal center.

In addition to its role in lymphoid tissues, expression of *FCRL3* in synovial tissue might explain the pathological connection between *FCRL3* variants and rheumatoid arthritis. *FCRL3* is strongly expressed in aggregated lymphocytes. Although our synovial samples showed only T-cell–B-cell aggregates, lymphocytes in rheumatoid arthritis synovial tissue are known to form a germinal center–like structure, called an ectopic germinal center, where T cell–dependent antibody production and affinity maturation occur[36]. Ectopic germinal-center formation also occurs in tissues from individuals with AITD and SLE, and *FCRL3* might be involved in pathological autoimmune reaction in these disease-specific ectopic lymphocyte aggregates.

Considering that augmented expression of *FCRL3* is associated with susceptibility to autoimmune disorders, and that *FCRL3* expression is regulated in B cells in the secondary lymphoid organ and is detected in lymphocytes of disease-specific tissues, *FCRL3* probably functions in immunity and potentially pathogenic in autoimmune disorders.

METHODS

Subjects. We enrolled three independent cohorts of individuals with rheumatoid arthritis (n = 830, 217 and 323), a cohort of individuals with SLE (n = 564) and a cohort of individuals with AITD (n = 509) comprising Graves' disease (n = 351) and Hashimoto's thyroiditis (n = 158) through several medical institutes in Japan. We recruited four independent cohorts of unaffected control subjects (n = 658, 262, 374 and 752) at various sites in Japan. All subjects were Japanese. Individuals with rheumatoid arthritis (84.2% women; age 59.0 ± 12.3 years (mean ± s.d.); 75.0% RF-positive) satisfied the revised criteria of the American Rheumatism Association for rheumatoid arthritis[47]. Individuals with SLE satisfied the criteria of the American College of Rheumatology for SLE[48]. Diagnosis of AITD was established on the basis of clinical findings and results of routine examinations for circulating thyroid hormone and thyroid-stimulating hormone concentrations, serum levels of antibodies against thyroglobulin, thyroid microsomes and thyroid-stimulating hormone receptors, ultrasonography, $^{[99m]}TCO_4^-$ (or $[^{123}I]$) uptake and thyroid scintigraphy.

We evaluated LD at 1q21–23 in the first control cohort compared with the first rheumatoid arthritis cohort to identify the rheumatoid arthritis–associated LD block and SNPs. The second and third rheumatoid arthritis and control cohorts were used for replication testing of results from the first cohorts. We tested Graves' disease; Hashimoto's thyroiditis; SLE; the combination of the two AITDs; and the combination of rheumatoid arthritis, SLE and the two AITDs for associations using the total pool of controls. We enrolled control subjects from three other ethnic groups, Korean (n = 100), African American (n = 120) and European American (n = 120), for evaluation of *FCRL3* haplotypes. We sampled synovial tissues from individuals with rheumatoid arthritis who underwent arthroplastic surgery. All subjects provided informed consent to participate in the study, as approved by the ethical committee of the SNP Research Center, RIKEN.

SNPs and genotyping. We identified SNPs in exons and 5′ and 3′ flanking regions of *FCRL1*, *FCRL2*, *FCRL3* and *FCRLψ4* by direct sequencing of DNA from 24 individuals. We selected other SNPs from the JSNP and Assay-On-Demand SNP databases (Applied Biosystems). We genotyped SNPs using Invader and TaqMan assays[41] as indicated by the manufacturers. Probe sets for the Invader assay were designed and synthesized by Third Wave Technologies, and those for the TaqMan assay were obtained from Applied Biosystems. When assessing the results of SNP genotyping, we generally excluded successful call rates <0.95 and values of $P < 0.01$ obtained by Hardy-Weinberg equilibrium testing in control subjects. The error rate of Invader assay was 0.0023, which was estimated by 11,092 assays in two replicates using 118 randomly selected SNPs (internal control data).

Luciferase assay. We cloned the promoter fragment of three haplotypes corresponding to nt −523 to +203 of *FCRL3* into the pGL3-Basic vector (Promega). We generated oligonucleotides using the allelic sequences of nt −189 to −160 of *FCRL3*. We cloned a single copy or four tandem copies of

these oligonucleotides into pGL3-Promoter vector (Promega). We grew Raji cells (RCB1647; RIKEN Cell Bank) in RPMI1640 medium supplemented with 10% fetal bovine serum and antibiotics. We electroporated (230 V and 975 μF) 1×10^7 cells with 5 pmol of constructs and 1 pmol of pRL-TK vector (internal control for transfection efficiency) in a 0.4-cm gap cuvette. After 48 h, we collected cells and measured luciferase activity using the Dual-Luciferase Reporter Assay System (Promega).

EMSA. We carried out EMSA and preparation of nuclear extract from Raji cells as previously described[49]. We labeled oligonucleotides −169T and −169C with digoxigenin-11-ddUTP using the DIG gel-shift kit (Roche). We incubated 5 μg of nuclear extract with 40 fmol of digoxigenin-labeled nucleotide for 25 min at room temperature. For competition experiments, we preincubated nuclear extract with unlabeled oligonucleotide (100-fold excess) before adding digoxigenin-labeled oligonucleotide. For supershift assays, we incubated 4 μg of antibodies to p50, p52, p65, RelB or cRel and rabbit IgG (control antibody; Santa Cruz Biotechnology) for 15 min at room temperature after incubation of the labeled probe. We separated protein-DNA complexes on a nondenaturing 6% polyacrylamide gel in 0.5× Tris-Borate-EDTA buffer. We transferred the gel to a nitrocellulose membrane and detected signals using an LAS-3000 luminoimage analyzer (Fujifilm).

RNA extraction and cDNA preparation. We collected peripheral blood from healthy volunteers to obtain $CD19^+$ lymphocytes. We separated polymorphonuclear cells by differential centrifugation using Lymphoprep resolving solution (AXIS-FIELD). We isolated $CD19^+$ lymphocytes using the MACS system with CD19 microbeads (Miltenyi Biotec) and confirmed that cell purity was >95% using flow cytometry. We stimulated cells with antibodies to CD40 (Cymbus Biotechnology) or IgM (Jackson Immunoresearch), with Il-4 (eBioscience), with APRIL (PeproTech), with BAFF (PeproTech) or with LPS (Sigma) for 4 h. We isolated total RNA using RNeasy Mini Kit (Qiagen). We quantified RNA in other normal tissues using Premium Total RNA (Clontech). We reverse-transcribed total RNA using TaqMan Gold RT-PCR reagents with random hexamers (Applied Biosystems) in accordance with the instructions of the manufacturer.

Quantification of *FCRL3* expression using real-time RT-PCR. We carried out real-time quantitative PCR using an ABI PRISM 7900 (Applied Biosystems) and Assay-on-Demand TaqMan probe and primers (Hs00364720_m1 for *FCRL3*) in accordance with the manufacturer's instructions. We generated a standard curve from the amplification data for *FCRL3* primers using a dilution series of total RNA from Raji cells as templates and normalized data to GUS level.

ASTQ. We carried out ASTQ as previously described[34] with some modifications. We prepared cDNA from B cells as described above. We amplified both cDNA and genomic DNA by PCR for 37 cycles using primers specific for exon 2 of *FCRL3* (**Supplementary Table 4** online) and for an additional cycle using forward primer with Alexa Fluor 488 label at the 5′ end. Products were directly digested using *Eag*I by incubation at 37 °C for 12 h. We monitored full digestion by the inclusion of PCR products from +358G/G homozygotes. We then separated digested products on a 12.5% polyacrylamide gel and quantified them using an LAS-3000 analyzer.

***In situ* hybridization and immunohistochemistry.** We carried out *in situ* hybridization as previously described[50]. We obtained probes from PCR products using the sequence of *FCRL3* (nt 2052–2490, comprising the intracellular unique region that is poorly conserved among members of this family). An additional probe of the 5′ untranslated sequence yielded similar results. We also examined control probes, which yielded no specific hybridization (data not shown). We used antibodies to CD3 (clone PS-1, Nichirei) and CD20 (clone L26, Zymed) for immunohistochemistry with an ABC Elite kit (Vector Labs) in accordance with the manufacturer's instructions. No specific staining was detected using mouse isotype IgG (data not shown).

Measurement of autoantibodies. We measured RF in sera of individuals with rheumatoid arthritis using latex-enhanced immunonephelometric assay. We measured antibody to DNA in sera of individuals with SLE by radioimmunoassay. Individuals with rheumatoid arthritis (n = 147, 81.1% women; age 63.9 ± 10.6 years (mean ± s.d.); 87.8% RF-positive; mean Steinbrocker radiographic stage 3.2) or SLE (n = 120, 92.6% women; age 36.6 ± 12.7 years (mean ± s.d.)) were part of the cohorts or from a single medical institute, respectively. For each individual, we used the maximum value of RF and antibody to DNA measured during the treatment period in the medical center or outpatient clinic. We detected antibody to CCP at a single time point using enzyme-linked immunosorbent assay, as previously described[38].

Statistical analysis. We calculated LD index Δ (ref. 28) and drew **Figure 1a** using Excel software (Microsoft). We estimated haplotype frequencies using HAPLOTYPER software. We applied the χ^2 test for contingency table tests for associations between allele-genotype distribution and phenotypes. *FCRL3* expression in B cells and autoantibody production were regressed on the number of susceptible alleles (coded 0, 1 and 2). All other statistical analyses, unless otherwise stated, were done using STATISTICA software (StatSoft).

URLs. The JSNP database is available at http://snp.ims.u-tokyo.ac.jp/index.html. TRANSFAC is available at http://www.gene-regulation.com/. HAPLOTYPER is available at http://www.people.fas.harvard.edu/~junliu/Haplo/docMain.htm.

GenBank accession number. *FCRL3* mRNA, NM_052939.

Note: Supplementary information is available on the Nature Genetics website.

ACKNOWLEDGMENTS

We thank E. Kanno and other members of the Laboratory for Rheumatic Diseases for technical assistance; H. Kawakami for expertise in computer programming; M. Yukioka, S. Tohma, Y. Nishioka, T. Matsubara, S. Wakitani, R. Teshima, N. Ishikawa, K. Ito, K. Ito, K. Kuma, H. Tamai and T. Akamizu for clinical sample collection; M. Ishikawa and Y. Amasaki for preparation of the second population study; M. Nagashima and S. Yoshino for sampling rheumatoid arthritis synovium; and K. Nagatani and Y. Komagata for advice. This work was supported by grants from the Japanese Millennium Project, the US National Institutes of Health and the Korean Molecular and Cellular BioDiscovery Research Program.

COMPETING INTERESTS STATEMENT

The authors declare that they have no competing financial interests.

Received 20 December 2004; accepted 25 February 2005
Published online at http://www.nature.com/naturegenetics/

1. Firestein, G.S. Evolving concepts of rheumatoid arthritis. *Nature* **423**, 356–361 (2003).
2. Gregersen, P.K., Silver, J. & Winchester, R.J. The shared epitope hypothesis. An approach to understanding the molecular genetics of susceptibility to rheumatoid arthritis. *Arthritis Rheum.* **30**, 1205–1213 (1987).
3. Newton, J.L., Harney, S.M., Wordsworth, B.P. & Brown, M.A. A review of the MHC genetics of rheumatoid arthritis. *Genes Immun.* **5**, 151–157 (2004).
4. Kochi, Y. *et al.* Analysis of single-nucleotide polymorphisms in Japanese rheumatoid arthritis patients shows additional susceptibility markers besides the classic shared epitope susceptibility sequences. *Arthritis Rheum.* **50**, 63–71 (2004).
5. Seldin, M.F., Amos, C.I., Ward, R. & Gregersen, P.K. The genetics revolution and the assault on rheumatoid arthritis. *Arthritis Rheum.* **42**, 1071–1079 (1999).
6. Tsao, B.P. The genetics of human systemic lupus erythematosus. *Trends Immunol.* **24**, 595–602 (2003).
7. Bowcock, A.M. & Cookson, W.O. The genetics of psoriasis, psoriatic arthritis and atopic dermatitis. *Hum. Mol. Genet.* **13** Suppl 1, R43–R55 (2004).
8. Marrack, P., Kappler, J. & Kotzin, B.L. Autoimmune disease: why and where it occurs. *Nat. Med.* **7**, 899–905 (2001).
9. Ueda, H. *et al.* Association of the T-cell regulatory gene CTLA4 with susceptibility to autoimmune disease. *Nature* **423**, 506–511 (2003).
10. Becker, K.G. *et al.* Clustering of non-major histocompatibility complex susceptibility candidate loci in human autoimmune diseases. *Proc. Natl. Acad. Sci. USA* **95**, 9979–9984 (1998).
11. Tokuhiro, S. *et al.* An intronic SNP in a RUNX1 binding site of SLC22A4, encoding an organic cation transporter, is associated with rheumatoid arthritis. *Nat. Genet.* **35**, 341–348 (2003).
12. Begovich, A.B. *et al.* A missense single-nucleotide polymorphism in a gene encoding a protein tyrosine phosphatase (PTPN22) is associated with rheumatoid arthritis. *Am. J. Hum. Genet.* **75**, 330–337 (2004).
13. Davis, R.S., Wang, Y.H., Kubagawa, H. & Cooper, M.D. Identification of a family of Fc receptor homologs with preferential B cell expression. *Proc. Natl. Acad. Sci. USA* **98**, 9772–9777 (2001).

14. Davis, R.S. *et al.* Fc receptor homologs: newest members of a remarkably diverse Fc receptor gene family. *Immunol. Rev.* **190**, 123–136 (2002).
15. Hatzivassiliou, G. *et al.* IRTA1 and IRTA2, novel immunoglobulin superfamily receptors expressed in B cells and involved in chromosome 1q21 abnormalities in B cell malignancy. *Immunity* **14**, 277–289 (2001).
16. Miller, I., Hatzivassiliou, G., Cattoretti, G., Mendelsohn, C. & Dalla-Favera, R. IRTAs: a new family of immunoglobulinlike receptors differentially expressed in B cells. *Blood* **99**, 2662–2669 (2002).
17. Xu, M.J., Zhao, R., Cao, H. & Zhao, Z.J. SPAP2, an Ig family receptor containing both ITIMs and ITAMs. *Biochem. Biophys. Res. Commun.* **293**, 1037–1046 (2002).
18. Ravetch, J.V. & Bolland, S. IgG Fc receptors. *Annu. Rev. Immunol.* **19**, 275–290 (2001).
19. Kyogoku, C. *et al.* Fcgamma receptor gene polymorphisms in Japanese patients with systemic lupus erythematosus: contribution of FCGR2B to genetic susceptibility. *Arthritis Rheum.* **46**, 1242–1254 (2002).
20. Capon, F. *et al.* Fine mapping of the PSORS4 psoriasis susceptibility region on chromosome 1q21. *J. Invest. Dermatol.* **116**, 728–730 (2001).
21. Dai, K.Z. *et al.* The T cell regulator gene SH2D2A contributes to the genetic susceptibility of multiple sclerosis. *Genes Immun.* **2**, 263–268 (2001).
22. Jirholt, J. *et al.* Genetic linkage analysis of collagen-induced arthritis in the mouse. *Eur. J. Immunol.* **28**, 3321–3328 (1998).
23. Sundvall, M. *et al.* Identification of murine loci associated with susceptibility to chronic experimental autoimmune encephalomyelitis. *Nat. Genet.* **10**, 313–317 (1995).
24. Teuscher, C. *et al.* Evidence that Tmevd2 and eae3 may represent either a common locus or members of a gene complex controlling susceptibility to immunologically mediated demyelination in mice. *J. Immunol.* **159**, 4930–4934 (1997).
25. Podolin, P.L. *et al.* Congenic mapping of the insulin-dependent diabetes (Idd) gene, Idd10, localizes two genes mediating the Idd10 effect and eliminates the candidate Fcgr1. *J. Immunol.* **159**, 1835–1843 (1997).
26. Nieto, A. *et al.* Involvement of Fcgamma receptor IIIA genotypes in susceptibility to rheumatoid arthritis. *Arthritis Rheum.* **43**, 735–739 (2000).
27. Radstake, T.R. *et al.* Role of Fcgamma receptors IIA, IIIA, and IIIB in susceptibility to rheumatoid arthritis. *J. Rheumatol.* **30**, 926–933 (2003).
28. Devlin, B. & Risch, N. A comparison of linkage disequilibrium measures for fine-scale mapping. *Genomics* **29**, 311–322 (1995).
29. Cordell, H.J. & Clayton, D.G. A unified stepwise regression procedure for evaluating the relative effects of polymorphisms within a gene using case/control or family data: application to HLA in type 1 diabetes. *Am. J. Hum. Genet.* **70**, 124–141 (2002).
30. Sebastiani, P. *et al.* Minimal haplotype tagging. *Proc. Natl. Acad. Sci. USA* **100**, 9900–9905 (2003).
31. Tsunoda, T. *et al.* Variation of gene-based SNPs and linkage disequilibrium patterns in the human genome. *Hum. Mol. Genet.* **13**, 1623–1632 (2004).
32. Pritchard, J.K., Stephens, M. & Donnelly, P. Inference of population structure using multilocus genotype data. *Genetics* **155**, 945–959 (2000).
33. Pritchard, J.K. & Rosenberg, N.A. Use of unlinked genetic markers to detect population stratification in association studies. *Am. J. Hum. Genet.* **65**, 220–228 (1999).
34. Kaijzel, E.L. *et al.* Allele-specific quantification of tumor necrosis factor alpha (TNF) transcription and the role of promoter polymorphisms in rheumatoid arthritis patients and healthy individuals. *Genes Immun.* **2**, 135–144 (2001).
35. Takemura, S. *et al.* Lymphoid neogenesis in rheumatoid synovitis. *J. Immunol.* **167**, 1072–1080 (2001).
36. Weyand, C.M. & Goronzy, J.J. Ectopic germinal center formation in rheumatoid synovitis. *Ann. N. Y. Acad. Sci.* **987**, 140–149 (2003).
37. Alarcon, G.S. *et al.* Suppression of rheumatoid factor production by methotrexate in patients with rheumatoid arthritis. Evidence for differential influences of therapy and clinical status on IgM and IgA rheumatoid factor expression. *Arthritis Rheum.* **33**, 1156–1161 (1990).
38. Suzuki, K. *et al.* High diagnostic performance of ELISA detection of antibodies to citrullinated antigens in rheumatoid arthritis. *Scand. J. Rheumatol.* **32**, 197–204 (2003).
39. Rantapaa-Dahlqvist, S. *et al.* Antibodies against cyclic citrullinated peptide and IgA rheumatoid factor predict the development of rheumatoid arthritis. *Arthritis Rheum.* **48**, 2741–2749 (2003).
40. Capon, F., Semprini, S., Dallapiccola, B. & Novelli, G. Evidence for interaction between psoriasis-susceptibility loci on chromosomes 6p21 and 1q21. *Am. J. Hum. Genet.* **65**, 1798–1800 (1999).
41. Suzuki, A. *et al.* Functional haplotypes of PADI4, encoding citrullinating enzyme peptidylarginine deiminase 4, are associated with rheumatoid arthritis. *Nat. Genet.* **34**, 395–402 (2003).
42. Barton, A. *et al.* A functional haplotype of the PADI4 gene associated with rheumatoid arthritis in a Japanese population is not associated in a United Kingdom population. *Arthritis Rheum.* **50**, 1117–1121 (2004).
43. Jorgensen, T.N., Gubbels, M.R. & Kotzin, B.L. New insights into disease pathogenesis from mouse lupus genetics. *Curr. Opin. Immunol.* **16**, 787–793 (2004).
44. Edwards, J.C. *et al.* Efficacy of B-cell-targeted therapy with rituximab in patients with rheumatoid arthritis. *N. Engl. J. Med.* **350**, 2572–2581 (2004).
45. Gray, D. *et al.* Observations on memory B-cell development. *Semin. Immunol.* **9**, 249–254 (1997).
46. van Eijk, M., Defrance, T., Hennino, A. & de Groot, C. Death-receptor contribution to the germinal-center reaction. *Trends Immunol.* **22**, 677–682 (2001).
47. Arnett, F.C. *et al.* The American Rheumatism Association 1987 revised criteria for the classification of rheumatoid arthritis. *Arthritis Rheum.* **31**, 315–324 (1988).
48. Hochberg, M.C. Updating the American College of Rheumatology revised criteria for the classification of systemic lupus erythematosus. *Arthritis Rheum.* **40**, 1725 (1997).
49. Aikawa, Y., Yamamoto, M., Yamamoto, T., Morimoto, K. & Tanaka, K. An anti-rheumatic agent T-614 inhibits NF-kappaB activation in LPS- and TNF-alpha-stimulated THP-1 cells without interfering with IkappaBalpha degradation. *Inflamm. Res.* **51**, 188–194 (2002).
50. Hoshino, M. *et al.* Identification of the stef gene that encodes a novel guanine nucleotide exchange factor specific for Rac1. *J. Biol. Chem.* **274**, 17837–17844 (1999).

EXTENDED REPORT

Up regulated expression of tumour necrosis factor α converting enzyme in peripheral monocytes of patients with early systemic sclerosis

T Bohgaki, Y Amasaki, N Nishimura, M Bohgaki, Y Yamashita, M Nishio, K-i Sawada, S Jodo, T Atsumi, T Koike

Ann Rheum Dis 2005;**64**:1165–1173. doi: 10.1136/ard.2004.030338

See end of article for authors' affiliations

Correspondence to: Dr Y Amasaki, Department of Medicine II, Hokkaido University Graduate School of Medicine, Address: N-15 W-7, Kita-ku, Sapporo 060-8638, Japan; yamasaki@med.hokudai.ac.jp

Accepted 28 December 2004

Background: Systemic sclerosis (SSc) is accompanied by abnormalities in humoral and cellular immune systems.

Objective: To determine the genes specifically expressed in the immune system in SSc by analysis of the gene expression profile of peripheral blood mononuclear cells (PBMC) from patients with SSc, including those treated with haematopoietic stem cell transplantation (HSCT). Additionally, to investigate the clinical significance of the up regulation of tumour necrosis factor α (TNFα) converting enzyme (TACE).

Methods: PBMC from patients with SSc (n = 23) and other autoimmune diseases (systemic lupus erythematosus (SLE, n = 16), rheumatoid arthritis (RA, n = 29)), and from disease-free controls (n = 36) were examined. Complementary DNA arrays were used to evaluate gene expression of PBMC, in combination with real time quantitative polymerase chain reactions. TACE protein expression in PBMC was examined by fluorescence activated cell sorter (FACS).

Results: In patients with SSc 118 genes were down regulated after HSCT. Subsequent comparative analysis of SSc without HSCT and healthy controls indicated SSc-specific up regulation for three genes: monocyte chemoattractant protein-3 ($p = 0.0015$), macrophage inflammatory protein 3α ($p = 0.0339$), and TACE ($p = 0.0251$). In the FACS analysis, TACE protein was mainly expressed on $CD14^+$ monocytes both in patients with SSc and controls. TACE expression on $CD14^+$ cells was significantly increased in patients with early SSc ($p = 0.0096$), but not in those with chronic SSc, SLE, or RA. TACE protein levels in SSc monocytes correlated with the intracellular CD68 levels ($p = 0.0016$).

Conclusions: Up regulation of TACE expression was a unique profile in early SSc, and may affect the function of TNFα and other immunoregulatory molecules.

Systemic sclerosis (SSc) is a multisystem disorder of connective tissue. Increased biosynthesis of multiple matrix proteins by interstitial fibroblasts is the hallmark of SSc, with development of skin sclerosis and involvement of visceral organs.[1] The pathogenesis of SSc includes vasculopathy associated with endothelial cell dysfunction, and extensive fibrosis secondary to fibroblast activation.[2 3] Functional abnormality in T and B lymphocytes has been considered in the pathogenesis, based on the presence of disease-specific autoantibodies and hypergammaglobulinaemia in SSc.[4 5] Growth factors and cytokines are also thought to play a part in the progression of connective tissue fibrosis in SSc. Among them, transforming growth factor β (TGFβ) and the Smad system have a central role in the SSc dermis.[6] However, the molecular basis of the pathogenesis of SSc has remained unclear.

The use of gene expression profiling, such as the complementary DNA (cDNA) array system, is increasingly being used for various diseases, and is used in the aetiological study of SSc.[7 8] Increased expression of several genes has been suggested, but a disease-specific gene profile of SSc has not yet been determined, possibly owing to the difficulty of achieving disease remission in SSc, which is necessary for a comparative analysis of the active and disease-free status. Recently, the efficacy of high dose chemotherapy after autologous haematopoietic stem cell transplantation (HSCT) for refractory autoimmune diseases has been reported.[9 10] HSCT has been performed in a number of cases of SSc, with good results.[11–13] When we performed autologous CD34 selected HSCT for our patients with SSc, we observed a prompt and persistent improvement of skin sclerosis and stabilisation of organ disease. Under this condition, it was possible to carry out a comparative analysis of gene expression profile between an active (pre-HSCT) and a remission status (post-HSCT) in the same patient with SSc.

We studied the gene expression profile in peripheral blood mononuclear cells (PBMC) from patients with SSc treated with HSCT, and found that expression of tumour necrosis factor α (TNFα) converting enzyme (TACE) was increased in circulating monocytes from patients with SSc. The correlation

Abbreviations: Ab, antibody; aCENP-B Ab, anticentromere protein-B Ab; ACR, American College of Rheumatology; ANA, antinuclear Ab; aRNP Ab, anti-ribonucleoprotein Ab; aTopo-I Ab, antitopoisomerase I Ab; CaMKIIβ, calcium/calmodulin dependent protein kinase II β; cDNA, complementary DNA; CRP, C reactive protein; CTGF, connective tissue growth factor; FACS, fluorescence activated cell sorter; FITC, fluorescein isothiocyanate; FSC, forward light scatter; GAPDH, glyceraldehyde-3-phosphate dehydrogenase; HSCT, haematopoietic stem cell transplantation; IL, interleukin; MCP, monocyte chemoattractant protein; MFI, mean fluorescence intensity; mIgG1, isotype matched control mouse IgG1; MIP, macrophage inflammatory protein; mRNA, messenger RNA; NF-κB, nuclear factor-κB; NIK, NF-κB inducing kinase; PBMC, peripheral blood mononuclear cells; PE, phycoerythrin; RA, rheumatoid arthritis; real time PCR, quantitative TaqMan real time polymerase chain reaction; RGS, regulators of G-protein signalling; SLE, systemic lupus erythematosus; SSc, systemic sclerosis; SSC, side light scatter; TACE, tumour necrosis factor α converting enzyme; TGFβ, transforming growth factor β; TNFα, tumour necrosis factor α; TNF-R, TNF receptor

Table 1 Clinical features of the study subjects*

Characteristics	SSc (n=20)	SSc treated with HSCT (n=3)	RA (n=29)	SLE (n=16)	Controls (n=36)
Sex (female/male)	17/3	2/1	23/6	14/2	25/11
Age (years), mean (SD)	51.0 (12.6)	43.3 (21.1)	58.9 (14.4)	40.5 (13.4)	40.0 (11.5)
Duration of disease (months), median (min–max)	41.0 (6–278)	18 (12–24)	36.0 (3–360)	144.0 (1–444)	
Prednisolone (mg/day), mean (min–max)	0.875 (0–10)	0.83 (0–2.5)	4.1 (0–25)	13.0 (0–60)	
Organ involvement, No (%)					
Lung	13 (65)	2 (67)	3 (10)	0 (0)	
Muscle	1 (5)	0 (0)	0 (0)	0 (0)	
Joint	8 (40)	0 (0)	29 (100)	3 (19)	
Renal	1 (5)	1 (33)	0 (0)	5 (31)	
Cardiac	2 (10)	0 (0)	0 (0)	0 (0)	
Serology, No (%)					
ANA	19 (95)	2 (67)	19 (66)	16 (100)	
αTopo-I Ab	11 (55)	2 (67)	N/A	N/A	
αCENP-B Ab	2 (10)	0 (0)	N/A	N/A	
αRNP Ab	1 (5)	0 (0)	N/A	11 (69)	

*The SSc groups consisted of 20 subjects, and three patients treated with HSCT. In these three patients with HSCT, RNA samples were obtained before (<1 month before mobilisation) and after HSCT.
Organ involvements in this study were defined as: lung (interstitial pneumonia proved by high resolution computed tomography), muscle (increased serum creatinine kinase or serum aldolase, or both, continuously), joint (arthralgia or arthritis, or both), renal (renal crisis in patients with SSc and nephritis in RA and SLE), cardiac (arrhythmia).[18–22]
N/A, not available.

of TACE expression with the clinical findings in patients with SSc was analysed and is discussed below.

PATIENTS AND METHODS

Patients and controls

Twenty three Japanese patients with SSc who fulfilled the 1980 criteria of the American College of Rheumatology (ACR) were assessed in this study.[14] These patients were categorised as those with diffuse cutaneous type disease characterised by generalised or widespread skin thickening.[15] Table 1 summarises their clinical features. Patients were classified as having early SSc (n = 12) if the disease duration after the appearance of the first non-Raynaud's phenomenon was within 3 years.[11] Other patients with SSc with a longer disease duration were classified as having chronic SSc (n = 11). Of the 12 patients with early SSc, three were treated with HSCT using autologous $CD34^+$ selected peripheral blood stem cells; blood samples were obtained throughout the clinical course. Other patients with autoimmune diseases had rheumatoid arthritis (RA) or systemic lupus erythematosus (SLE). These patients fulfilled the criteria of the ACR, respectively.[16 17] As healthy controls, 36 disease-free Japanese volunteers, mean (SD) age 40.0 (11.5) years, were enrolled in the study.

Study design

To search for specific genes which changed between the active and remission status, before and after HSCT, we first analysed gene expression profiles of PBMC from patients treated with HSCT using cDNA array (n = 3). Next, specific up regulated genes in patients with SSc were explored using cDNA array by comparing mRNA levels in PBMC of patients with SSc who had not received HSCT (n = 6) and healthy controls (n = 5). Specific gene candidates were confirmed by real time polymerase chain reaction (PCR) in patients with SSc without HSCT (n = 9) and controls (n = 6). Finally, protein expression levels were analysed by a fluorescence activated cell sorter (FACS) analysis.

PBMC isolation

Blood sampling was carried out after obtaining written informed consent according to the guidelines of the ethical committee of Hokkaido University. PBMC were obtained from heparinised venous blood, using gradient centrifugation over Ficoll-Paque Plus (Amersham Biosciences Corp, NJ).

RNA extraction and cDNA array analysis

Total RNAs from PBMC were isolated using TRIzol reagent (Invitrogen, Carlsbad, CA). Poly(A) RNA was isolated from total RNA using a MagExtractor (TOYOBO, Osaka, Japan), and poly(A) RNA (2 μg) was reverse transcribed by ReverTraAce (TOYOBO), in the presence of cDNA synthesis primers and biotin-16-deoxyuridine triphosphate (TOYOBO), according to the manufacturer's instructions. cDNA array analysis was performed using human cDNA expression filters (Human Immunology Filters (TOYOBO)), on which 621 species of human cDNA fragments and housekeeping genes are spotted in duplicate: (http://www.toyobo.co.jp/seihin/xr/product/genenavi/genenavigator.html, accessed 5 May 2005)). Hybridisation and subsequent cDNA array analyses were carried out as described previously,[23] with some modification. Briefly, after standard prehybridisation, cDNA array filters were hybridised with a biotin labelled cDNA probe in PerfectHyb solution (TOYOBO) overnight at 68°C. After washing under conditions of high stringency, specific signals on the filters were visualised using Phototope-Star Detection Kits (New England Biolabs, Beverly, MA). Fluorescence signals for mRNA expression levels were obtained using a Fluor-S Multiimager system (Nippon Bio-Rad Laboratories, Tokyo, Japan). The signal intensity among filters was compared in an E-Gene Navigator Analysis (GeneticLab, Sapporo, Japan), and was expressed as an mRNA expression index to the intensity of the internal glyceraldehyde-3-phosphate dehydrogenase (GAPDH) gene expression.

Quantitative TaqMan real time polymerase chain reaction (real time PCR)

A two step PCR was carried out on serial dilutions of cDNA samples from PBMC from the patients with SSc and the controls. Real time PCR amplification and determination of cDNA transcripts were carried out with the ABI PRISM 7000 sequence detection system (Applied Biosystems, Foster City, CA) and gene-specific sets of TaqMan Universal PCR master mix and assays-on-demand gene expression probes (Applied Biosystems).

Table 2 Down regulated genes expressed in PBMC from patients with SSc at 6 months after HSCT as indicated by a cDNA array

Gene name	Accession No	Gene name	Accession No	Gene name	Accession No
Bik	X89986	MCP-2	Y16645	GRP94	X15187
Caspase-8	U60520	MCP-3	X72308	HSP105β	AB003333
JunB	X51345	Neurophysin II	X03172	MMP3	J03209
AP-β	X95694	Delta	AF003522	TACE	U86755
AP-γ	X95693	Angiotensinogen	K02215	Cathepsin G	M16117
Erg-1	M21535	Gonadotropin α peptide	V00518	Pin1	U49070
GLI-3	M57609	Somatostatin	J00306	Calpastatin	U26724
IκBα	M69043	VIP	M36634	Moesin	M69066
IRF-2	X15949	Gastrin	V00511	Radixin	L02320
N-Myc	M13228	IP10	X02530	LAT	AF036905
Per2	AB002345	MIP-3α	U77035	Fyb	AF001862
Pax5	M96944	EphA5	L36644	Furin	X17094
LXRα	U22662	EphB6	D83492	PAI-2	M16006
RXRγ	U38480	Insulin receptor	M10051	CD3γ	X04145
RAC3	AF010227	MC1-R	X67594	CD3ε	X03884
PPARγ	L40904	MC4-R	L08603	CD3ζ	J04132
MCR	M16801	β2-AR	M15169	CD8β 1	X13444
MEK-5	U25265	FRP-3	U24163	CD5	X04391
MEK kinase-2	AF111105	Notch 2	AF097645	CD72	M54992
Raf-1	X03484	Thrombin R	M62424	CD6	X60992
Raf-B	M95712	IFNγR2	U05875	CD7	X06180
KKIAMRE	U35146	IL2Rγ	D11086	CD20	X12530
Rhotekin	AI970663	IL15Rα	U31628	CD27	M63928
IKKα	AF080157	c-Kit	X06182	CD28	J02988
JAK1	M64174	CXCR-4	AF025375	CD35	Y00816
MuSK	AF006464	Slap	D89077	CD38	M34461
TGFβ2	M19154	Shb	X75342	CD40L	L07414
GDF-8	AF019627	Sos1	L13858	CD42a	X52997
Inhibin α	M13981	Dbl	J03639	CD43	J04168
FGF-1	X51943	Ral GDS	U14417	CD46 BC1	M58050
FGF-5	M37825	RGS4	U27768	CD59	X16447
FGF-6	X63454	PI4-Kα	AJ011121	CD69	L07555
HGF β chain	E08541	FRP1	U49844	CD74	X03339
IGF-BP3	M35878	Som68	M88108	TCRα	U36759
TNFβ	D12614	PPP1CA	X70848	TCRβ	L07294
IL2	U25676	CD45	Y00062	TCRγ	Y00790
IL10	M57627	p120	AF062343	CD138	J05392
IL15	AF031167	Ref-1	D90373	ICAM3	X69819
IL18	D49950	HSP60	M34664		
SCF	M59964	HSP90β	M16660		

One hundred and eighteen gene expressions decreased more than 20% in all three patients with SSc treated with HSCT at 6 months after HSCT compared with before HSCT (<1 month before mobilisation) by cDNA array analysis. Changes in white blood cell and monocyte counts in PBMC from three patients with SSc treated with HSCT were from 4867 (116)/μl to 5100 (917)/μl ($p=0.5105^*$) and from 506 (157)/μl to 589 (44) /μl ($p=0.7106^*$), respectively. *Paired *t* test.

FACS analysis

The following mouse monoclonal antibodies were purchased from BD Biosciences Pharmingen (San Diego, CA): anti-human CD3-Cy-chrome, CD4-fluorescein isothiocyanate (FITC), CD8-phycoerythrin (PE) and FITC, CD56-FITC, CD19-FITC, CD68-PE, and CD69-PE. Monoclonal mouse antihuman-CD14-FITC, CD71-PE (Beckman Coulter Inc, Fullerton, CA) and antihuman TACE-PE (R&D systems, Abingdon, UK) were also used for surface immunostaining of the cells. The specificity of antihuman TACE has been characterised.[24] In the case of CD68, intracellular staining was done using Cytofix/Cytoperm Plus (BD Biosciences Pharmingen, San Diego, CA), according to the manufacturer's instructions. After washing twice with phosphate buffered saline (PBS), cells were subjected to FACS analysis of immunostained cells using a FACSCalibur flow cytometer (Becton Dickinson Immunocytometry Systems, San Jose, CA).

Statistical analysis and clinical significance

Calculations were made using the statistical software package StatView 5.0 (Abacus Concepts, Berkeley, CA). Comparisons of mRNA expression of PBMC were made using Mann-Whitney statistics. Group mean comparisons of the TACE protein expression levels, represented by mean fluorescence intensity (MFI), and TACE positive cells were based on Kruskal-Wallis H statistics. A paired *t* test was used to analyse the difference in blood cell counts of patients with SSc before and after HSCT. The data are presented as the means (SD). Differences were examined based on analysis of variance, and p values <0.05 were considered significant.

RESULTS

Comprehensive analysis of up regulated genes in PBMC from patients with SSc using cDNA array and real time PCR

We first analysed mRNA expression in PBMC from three patients with SSc treated with HSCT, in order to search for genes with expression levels down regulated after this treatment. In these patients, skin involvement, as expressed by the modified Rodnan total thickness skin score improved significantly by 54% (from 30.3 (6.8) to 12.6 (13.2)) and the modified Health Assessment Questionnaire improved by 22.8% (from 1.67 (0.88) to 1.29 (1.04)) at 6 months after effective HSCT. This improvement persisted even 3 years after this treatment. PBMC specimens were obtained from these patients before (<1 month before mobilisation) and 6 months after HSCT, and were processed for mRNA extraction followed by cDNA array analyses.

Table 3 Up regulated genes expressed in PBMC from patients with SSc without HSCT as indicated by a cDNA array

Classification	Up regulated genes	GenBank accession No	Ratio (fold increase)
Regulatory transcription factors	Per1	AB002107	7.61
	Erg-3	S40832	4.50
	Gfi-1	U67369	4.44
Protein kinases	CaMKIIβ	AF078803	4.90
Growth factors and hormones	IL1β*	X02532	9.70
	MIP-1β*	J04130	6.58
	TARC	D43767	5.56
	IL12p35	AF180562	4.27
	MIP-3α*	U77035	4.25
	MCP-3*	X72308	3.88
Membrane receptors	IL15Rα	U31628	3.46
Signalling intermediates	Gab1	U43885	6.09
	RGS-1*	X73427	5.21
	Shb	X75342	4.32
	TACE*	U86755	3.70
	Dbl	J03639	3.38
Lymphocyte signalling	CD34	M81104	3.40

The ratio of the gene expression index (see "Patients and methods") of patients with SSc without HSCT (n=6) to healthy controls (n=5) was calculated, and the list of up regulated genes using cDNA array (with an SSc/control ratio >3.0) is displayed. *Gene expression was confirmed by real time PCR.
CaMKIIβ, calcium/calmodulin dependent protein kinase II β; MIP-1β, macrophage inflammatory protein β; MCP-3, monocyte chemoattractant protein-3; RGS-1, regulators of G-protein signalling-1.

At 6 months after this treatment, down regulation of mRNA expression levels was seen in 118 genes using cDNA array (table 2). In patients with SSc without HSCT, 17 genes were specifically up regulated compared with controls (table 3). In addition, the profile of mRNA expression between baseline and after 6 months in patients with SSc without HSCT was very similar, thus a "natural state for 6 months" did not modify the mRNA levels examined in this study (data not shown). Real time PCR showed that only four gene expression levels had statistical significance as disease-specific genes in 17 patients with SSc who had not received HSCT (fig 1). As a result, gene expression levels of monocyte chemoattractant protein (MCP)-3, macrophage inflammatory protein (MIP)-3α, and TACE were down regulated after HSCT in the cDNA array and up regulated specifically in patients with SSc without HSCT by real time PCR (fig 2). In this study, we further investigated the expression of TACE, which has a crucial role in the immune system. A role for chemokines, including MCP and MIP families, in the pathogenesis of scleroderma has been suggested (reviewed by Atamas and White[25]).

Cell surface TACE expression

We first examined PBMC from healthy controls for the expression of TACE protein. In PBMC from healthy subjects, a small population was brightly stained by an antihuman TACE monoclonal antibody (fig 3A). Multicolour FACS analyses showed that surface TACE expression was barely detectable on $CD4^+CD3^+$, $CD8^+CD3^+$, $CD19^+$, and $CD56^+$ populations. In contrast, surface TACE expression was detected on the $CD14^+$ population (fig 3B). It was confirmed that these $CD14^+$ populations were monocytes, by profiles of forward and side light scatter (SSC), as well as by intracellular CD68 protein expression. Surface TACE expression levels on monocytes were not affected by the age and sex of the controls (data not shown).

We next investigated expression levels of TACE protein in subsets of PBMC from patients with SSc. In these patients, surface TACE expression was also detected on monocytes but not on $CD4^+CD3^+$, $CD8^+CD3^+$, $CD19^+$, and $CD56^+$ populations, respectively (data not shown). Figure 3C shows representative FACS profiles of TACE protein expression for $CD14^+$

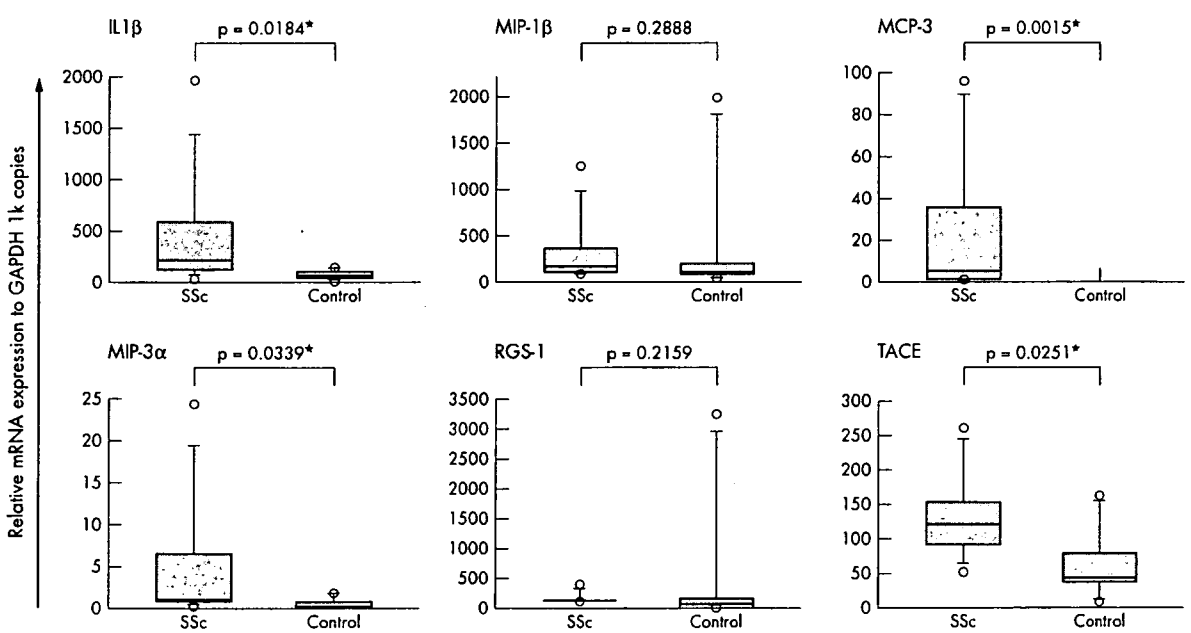

Figure 1 Quantitative analysis of up regulated genes in PBMC from patients with SSc, assessed using real time PCR. cDNA specimen from patients with SSc (n=9) and disease-free volunteers (n=6) were analysed for six genes species (TACE, interleukin (IL) 1β, MIP-3α, MIP-1β, MCP-3, and a regulator of G-protein signalling (RGS)-1), indicated from the cDNA array study (table 3). *p<0.05.

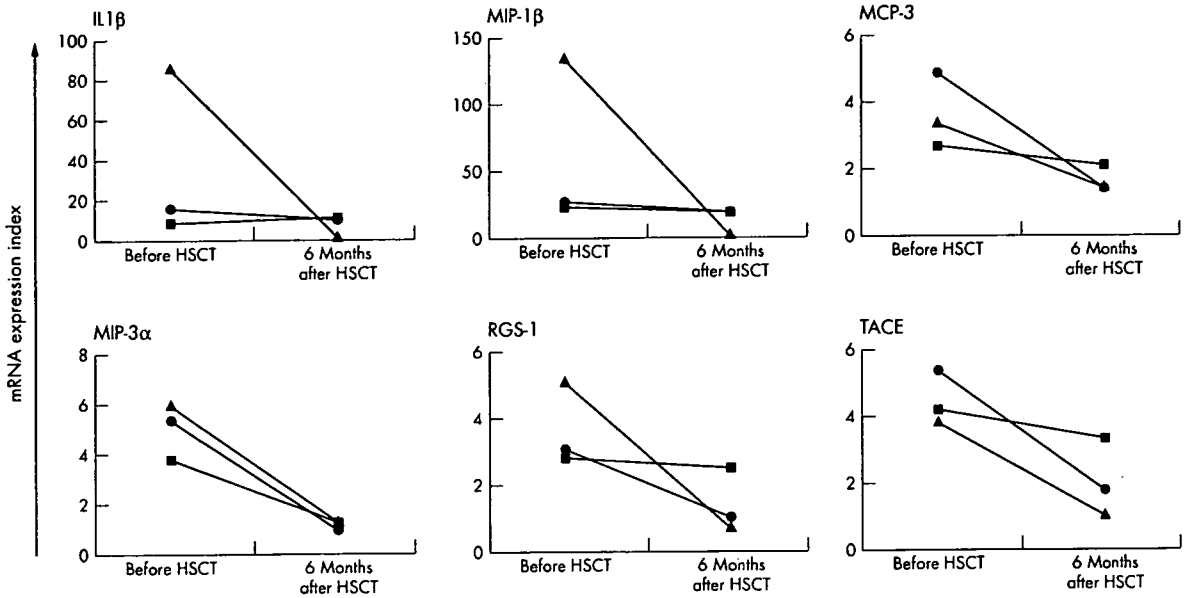

Figure 2 Changes of mRNA expression levels of IL1β, MIP-1β, MCP-3, MIP3-α, RGS-1, and TACE in patients with SSc before and after HSCT using cDNA array. RNA specimens were obtained from individual patients before (<1 month before mobilisation) and 6 months after HSCT. Relative expression levels of mRNA were determined using cDNA arrays performed simultaneously. The expression levels of each cDNA transcript were displayed as a relative mRNA expression index compared with the levels of internal GAPDH gene expression, as described in "Patients and methods".

monocytes. In the patients with SSc, TACE expression in monocytes was significantly increased in comparison with findings in healthy controls, and in patients with RA and SLE (fig 3C). When analysed statistically, cell surface TACE protein levels of monocytes and TACE positive cells in peripheral blood were significantly increased in patients with SSc, especially in patients with early SSc with disease duration of <3 years, in comparison with controls and patients with non-SSc autoimmune diseases, as well as those with chronic SSc (fig 4). In addition, TACE protein levels correlated with mRNA expression levels by real time PCR ($r = 0.640$, $p = 0.0462$). Thus, we concluded that up regulated expression of TACE protein by monocytes was a unique profile of early SSc.

Relationship between cell surface TACE expression and maturation/activation markers of monocytes

To better understand the mechanism of TACE up regulation in monocytes in SSc, we next investigated correlations between TACE and activation/differentiation markers of monocytes from patients with SSc. Coexpression of surface CD69, CD71, and intracellular CD68 with TACE was evaluated using FACS analysis (fig 5). These proteins were variously expressed on SSc monocytes, but only intracellular CD68 protein levels showed a significant correlation with cell surface TACE protein expression levels ($r = 0.671$, $p = 0.0016$), while cell surface CD69 and CD71 proteins did not correlate.

Association of cell surface TACE expression levels with clinical features of SSc

We then analysed the correlation of cell surface TACE protein levels of monocytes from patients with SSc (including patients with early and chronic disease) with clinical features of the disease. The expression levels of TACE protein on monocytes in patients with SSc, however, did not significantly correlate with titres of autoantibodies, including antinuclear Ab (ANA), antitopoisomerase I Ab (aTopo-I Ab), anticentromere protein-B Ab (aCENP-B Ab), anti-ribonucleoprotein Ab (aRNP Ab), as well as levels of serum immunoglobulins. The TACE protein levels did not correlate either with CRP in patients with SSc (fig 4, $r = -0.216$, $p = 0.3599$). The expression levels of TACE protein did not differ significantly between patients with SSc with or without visceral organ disease, including interstitial pneumonia and gastrointestinal complications (data not shown).

DISCUSSION

HSCT can be an effective treatment for subjects with severe autoimmune diseases, including SSc.[11–13] In our three patients with SSc who received HSCT, significant improvement of skin sclerosis was promptly achieved and persisted without any immunosuppressant drug treatment. In such patients, the gene expression profile can be studied comparatively between the active and remission state of SSc, with a minimum background of therapeutic reagents. In this study we performed a cDNA analysis of PBMC from patients with SSc who had undergone HSCT. After extensive analyses, up regulation of MCP-3, MIP-3α, and TACE in PBMC from patients with SSc who had not had HSCT was evident.

It was notable that these genes are commonly expressed by monocytes/macrophages. In SSc, although the earliest pathological events include dysfunction of microvascular systems and dermal fibroblasts,[26 27] cells and factors that mediate such abnormalities have not been defined. Histological studies of early SSc showed that cells infiltrating the skin of patients with early stage SSc are mainly $CD14^+$ monocytes/macrophages,[28 29] indicating the crucial role of these cells.

A role for chemokines has been suggested in the pathogenesis of SSc.[25 30–32] Our observation about MCP-3 and MIP-3α in PBMC from patients with SSc in this study is consistent with previous findings.[33–35]

In addition, overexpression of TACE in PBMC appeared to be a new hallmark of early stage SSc. In PBMC subpopulations, TACE protein expression was almost limited to

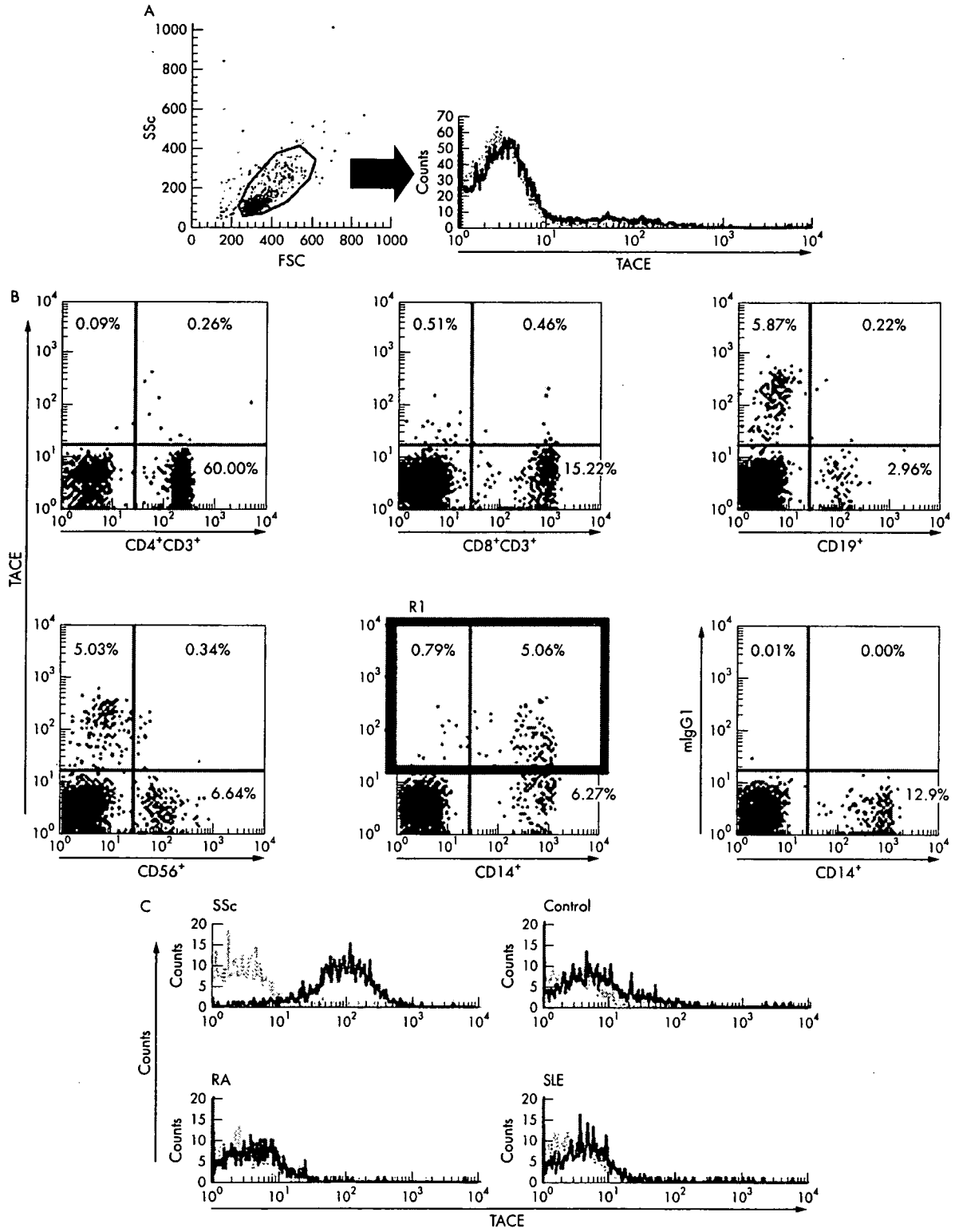

Figure 3 Expression of TACE protein in PBMC of healthy controls and patients. (A, left panel) A small population was detected in a high fluorescence intensity. (A, right panel) Solid line, cells stained with anti-TACE monoclonal Ab; dotted line, cells stained with isotype matched control mouse IgG1 Ab. (B) Expression of TACE protein in PBMC subsets from a healthy control. (C) Representative cell surface expression of TACE protein on monocytes from patients with autoimmune diseases and controls. Solid line, cells stained with anti-TACE monoclonal Ab; dotted line, cells stained with mIgG1 Ab. Results are representative of three independent experiments.

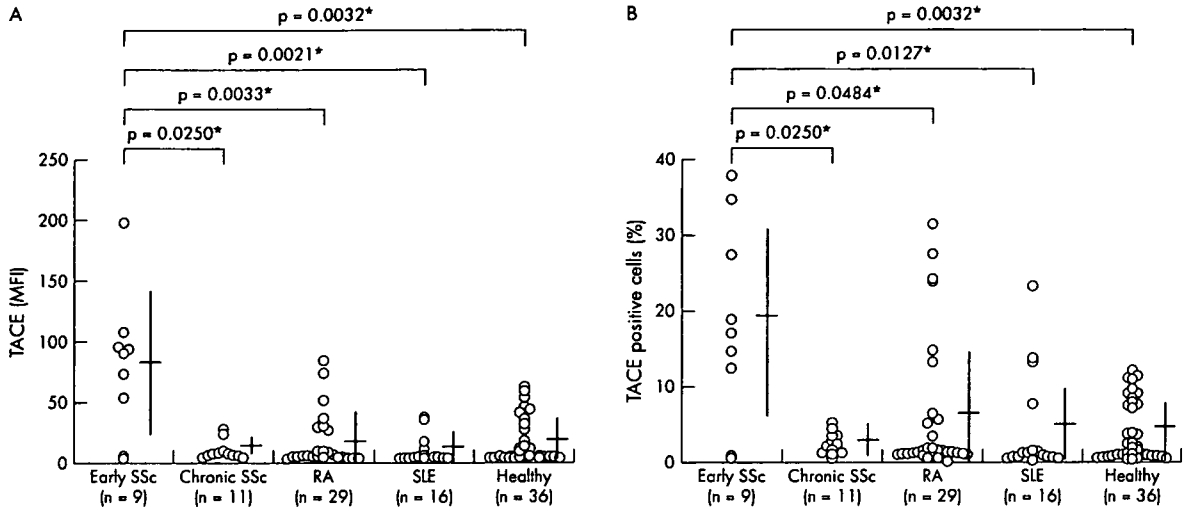

Figure 4 (A) Comparison of cell surface TACE expression by monocytes of patients with early SSc, chronic SSc, RA, SLE, and healthy controls. Cell surface expression levels of TACE were evaluated using FACS, gating on monocytes by forward and side light scatter and on $CD14^+$ cells. The levels of TACE protein expression were represented by the MFI. mIgG1 Ab-PE staining was performed in all measurements, and showed identical levels of background staining. *$p<0.05$, ($p=0.0065$ (Kruskal-Wallis H statistics)). (B) Comparison of TACE positive cells in PBMC of patients with early SSc, chronic SSc, RA, SLE, and healthy controls evaluated using FACS. TACE positive cells were defined on gate R1 in fig 3B. *$p<0.05$.

monocytes (fig 3B), whereas widespread distribution of TACE mRNA in tissue was suggested and its expression of protein levels in blood cells has not been yet described in detail.[36 37] TACE protein levels on monocytes were significantly higher in SSc than in controls (figs 3C and 4), suggesting a possible association between TACE and the function of TACE-expressing monocytes with the pathoaetiology of SSc. In autoimmune diseases, up regulation of TACE in inflammatory synovial tissue from patients with RA and increased TACE mRNA expression in PBMC of patients with multiple sclerosis have been suggested, but the disease specificity has been unclear.[38–40] Our report provides the first

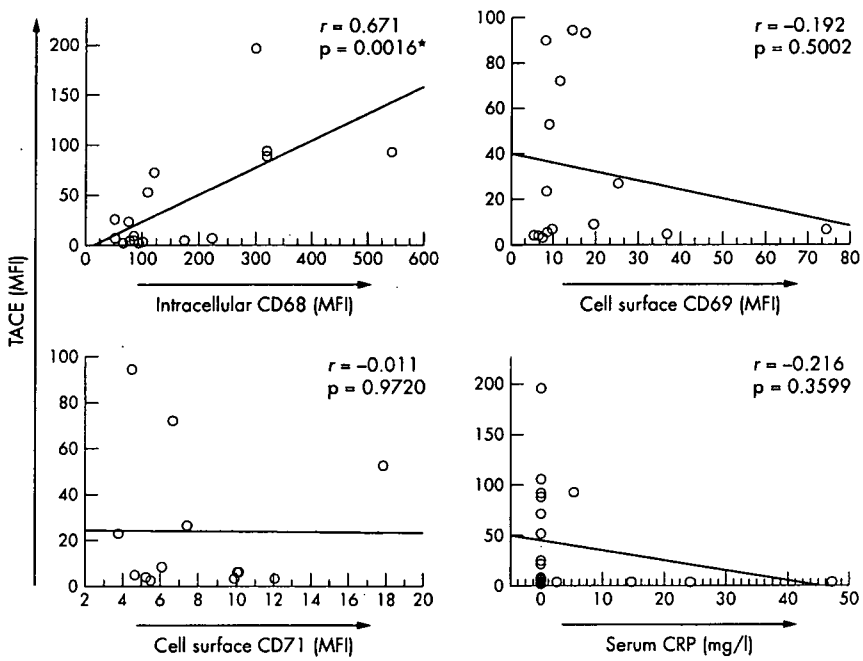

Figure 5 Correlation of TACE protein expression levels and maturation/activation markers on monocytes, and serum CRP levels in patients with SSc. Correlation of TACE protein levels with intracellular CD68 expression, cell surface CD69 expression, cell surface CD71 expression, and serum C reactive protein (CRP) levels are displayed. Cells were stained with anti-TACE-PE monoclonal antibody, or with FITC-anti-CD68, CD69, and CD71, in the presence of anti-CD14-FITC. Intracellular or cell surface levels of each marker were measured by FACS, gating on the monocytes as described above. The expression levels of individual proteins, represented by the MFI, were plotted on the horizontal axis (CD68, CD69, and CD71) and on the vertical axis (TACE), respectively. Serum CRP levels were measured by a latex agglutination test. *$p<0.05$.

evidence of disease-specific up regulation of TACE in peripheral monocytes in SSc, both at mRNA and protein expression levels.

TACE is a metalloproteinase of the ADAM (a disintegrin and metalloproteinase) family, and was initially described as a protease responsible for processing the membrane anchored TNFα precursor to the mature secreted form.[36 37] It is now accepted that substrates of TACE also include various cell surface proteins other than pro-TNFα; TNF receptors type I (TNF-RI) and type II (TNF-RII), L-selectin, IL6 receptor α chain, TNF related activation induced cytokine, and fractalkine (reviewed by Mezyk *et al*[41]). TACE mRNA is expressed by various types of cells, and can be induced by various extracellular stimuli.[41 42] We found that expression of TACE increased at mRNA levels in PBMC from patients with SSc (table 3, fig 1). Moreover, expression levels of TACE protein correlated with that of intracellular CD68, a lysosomal antigen expressed during differentiation of monocytes to macrophages, and did not correlate with CD69, CD71, activation markers in blood cell, and CRP levels (fig 5).[43] In patients with RA with positive CRP, surface TACE protein levels in peripheral monocytes also had no correlation ($r = -0.277$, $p = 0.1459$). Monocytes from patients with early stage SSc were likely to be activated in vivo, expressing TACE, independently of general acute reactants. Expression of TACE mRNA is regulated by transcription factors, including AP-2 and SP-1.[44] Analysis of these factors may help in understanding the mechanism of TACE up regulation.

It was notable that TACE up regulation in monocytes was not seen in patients with chronic SSc with diffuse skin sclerosis (fig 4). Hence, up regulation of TACE in circulating monocytes was probably not a secondary outcome from a persistent fibrotic condition. In the pathogenesis of SSc, TGFβ and connective tissue growth factor (CTGF) dysfunction has been considered.[8 45] In addition, the up regulated TNFα/TNF-R system has also been suggested in recent studies. It has been reported that the serum soluble TNF-R levels significantly correlated with the activity and disease progression of SSc.[46 47] Furthermore, Ellman and MacDonald reported a significant improvement in the skin score of patients with SSc after administration of recombinant anti-TNFα antibody.[48] These findings are consistent with involvement of an aberrant function of the TNFα/TNF-R system in SSc. The up regulation of TACE may be involved in such abnormality in TNF signalling in SSc through the cleaving function of TACE.

The effect of TACE on the function of the TNFα/TNF-R system in vivo is not fully understood, but the soluble form of TNFα can interact with both TNF-RI and TNF-RII.[49–51] Ligation of TNF-RI leads to recruitment of intracellular signalling proteins, resulting in the bifurcation of TNF-RI signalling: one is the apoptotic signal delivered through caspase-8, and the other is activation of proinflammatory properties delivered through nuclear factor-κB (NF-κB) inducing kinase (NIK) and NF-κB.[52] Unlike TNF-RI, signalling through TNF-RII largely leads to activation of NIK dependent and NF-κB dependent signalling.[53] Thus, increased activity of TACE can shift the balance of signals mediated by distinct types of TNF receptors and downstream events, including activation or death of target cells. Interestingly, mice with a targeted mutation in TACE were perinatally lethal and had morphological defects in the skin, indicating the essential role of TACE in normal skin development.[54]

Thus, it is intriguing to consider that TACE may participate in the progression of skin involvement in SSc, especially at the early stage. However, TNFα can also down regulate the expression of CTGF and indirectly modulate expression of type II TGFβ receptor in human fibroblasts.[55 56] In addition, TACE can also cleave other functional molecules as well as TNFα and the receptors.[41] Such pleiotrophic action of TACE makes it difficult to predict a bona fide role of TACE up regulation in SSc. Further investigation of the function of TACE, including analysis of laboratory animals that overexpress TACE, may provide information about the significance of TACE in SSc.

In summary, this study described for the first time the aberrant expression of TACE on monocytes from patients with early SSc. Recently, several chemical compounds have been reported to inhibit the activities of metalloproteinases, including TACE.[57] Such reagents may have a role in cases of TACE associated chronic inflammatory disease, including SSc. In addition, expression of TACE levels may also be a useful clinical measure of SSc, reflecting disease stages and the clinical prognosis of individual patients. Analysis of TACE function in SSc monocytes may not only provide insight into the pathogenesis but may also be a new diagnostic and therapeutic target for SSc.

ACKNOWLEDGEMENTS

We thank Ms Akiko Hirano for expert technical assistance, Drs Hiroshi Kataoka, Akira Furusaki, Katsuya Fujimoto, and Tomoyuki Endo for clinical procedures related to HSCT.

This work was supported by a national grant aid (14570004) from the Ministry of Education, Science, Technology, Sports, and Culture of Japan and a research grant for the study of the action of short fatty chain acid on cytokine gene regulation.

Authors' affiliations

T Bohgaki, Y Amasaki, M Bohgaki, Y Yamashita, M Nishio, S Jodo, T Atsumi, T Koike, Department of Medicine II, Hokkaido University Graduate School of Medicine, N-15 W-7, Kita-ku, Sapporo 060-8638, Japan

N Nishimura, GeneticLab Co, Ltd, N-27 W-6, Kita-ku, Sapporo 001-0027, Japan

K-i Sawada, Department of Internal Medicine III, Akita University School of Medicine, 1-1-1 Hondo, Akita 010-8543, Japan

REFERENCES

1 **Wigley FM**, Hummers LK. Systemic sclerosis. In: Hochberg MC, Silman AJ, Smolen JS, Weinblatt ME, Weisman MH, eds. *Rheumatology*.3rd ed. Edinburgh, UK: Mosby, 2003:1455–522.
2 **Furst DE**, Clements PJ. Hypothesis for the pathogenesis of systemic sclerosis. *J Rheumatol* 1997;**24**(suppl 48):53–7.
3 **Sakkas LI**, Platsoucas CD. Is systemic sclerosis an antigen-driven T cell disease? *Arthritis Rheum* 2004;**50**:1721–33.
4 **Sakkas LI**, Xu B, Artlett CM, Lu S, Jimenez SA, Platsoucas CD. Oligoclonal T cell expansion in the skin of patients with systemic sclerosis. *J Immunol* 2002;**168**:3649–59.
5 **Saito E**, Fujimoto M, Hasegawa M, Komura K, Hamaguchi Y, Kaburagi Y, *et al*. CD19-dependent B lymphocyte signalling thresholds influence skin fibrosis and autoimmunity in the tight-skin mouse. *J Clin Invest* 2002;**109**:1453–62.
6 **Varga J**. Scleroderma and Smads: dysfunctional Smad family dynamics culminating in fibrosis. *Arthritis Rheum* 2002;**46**:1703–13.
7 **Zhou X**, Tan FK, Xiong M, Milewicz DM, Feghali CA, Fritzler MJ, *et al*. Systemic sclerosis (scleroderma): specific autoantigen genes are selectively overexpressed in scleroderma fibroblasts. *J Immunol* 2001;**167**:7126–33.
8 **Luzina IG**, Atamas SP, Wise R, Wigley FM, Choi J, Xiao HQ, *et al*. Occurrence of an activated, profibrotic pattern of gene expression in lung CD8+T cells from scleroderma patients. *Arthritis Rheum* 2003;**48**:2262–74.
9 **Burt RK**, Traynor AE, Craig R, Marmont AM. The promise of haematopoietic stem cell transplantation for autoimmune diseases. *Bone Marrow Transplant* 2003;**31**:521–4.
10 **Tyndall A**, Passweg J, Gratwohl A. Haematopoietic stem cell transplantation in the treatment of severe autoimmune diseases 2000. *Ann Rheum Dis* 2001;**60**:702–7.
11 **Binks M**, Passweg JR, Frust D, McSweeney P, Sullivan K, Besenthal C, *et al*. Phase I/II trial of autologous stem cell transplantation in systemic sclerosis: procedure related mortality and impact on skin disease. *Ann Rheum Dis* 2001;**60**:577–84.
12 **Tyndall A**, Koike T. High-dose immunoablative therapy with haematopoietic stem cell support in the treatment of severe autoimmune disease: current status and future direction. *Intern Med* 2002;**41**:608–12.
13 **Farge D**, Passweg J, van Laar JM, Marjanovic Z, Besenthal C, Finke J, *et al*. Autologous stem cell transplantation in the treatment of systemic sclerosis: report from the EBMT/EULAR registry. *Ann Rheum Dis* 2004;**63**:974–81.
14 **ARA**. Preliminary criteria for the classification of systemic sclerosis (scleroderma). Subcommittee for scleroderma criteria of the American

Rheumatism Association Diagnostic and Therapeutic Criteria Committee. *Arthritis Rheum* 1980;**23**:581–90.
15 **LeRoy EC**, Krieg T, Black C, Jablonska S, Krieg T, Medsger TA Jr, *et al.* Scleroderma (systemic sclerosis); classification, subsets and pathogenesis. *J Rheumatol* 1988;**15**:202–5.
16 **Arnett FC**, Edworthy SM, Bloch DA, McShane DJ, Fries JF, Cooper NS, *et al.* The American Rheumatism Association 1987 revised criteria for the classification of rheumatoid arthritis. *Arthritis Rheum* 1998;**31**:315–24.
17 **Hochberg MC**. Updating the American College of Rheumatology revised criteria for the classification of systemic lupus erythematosus. *Arthritis Rheum* 1997;**40**:1725.
18 **Warrick JH**, Bhalla M, Schabel SI, Silver RM. High resolution computed tomography in early scleroderma lung disease. *J Rheumatol* 1991;**18**:1520–8.
19 **Clements PJ**, Furst DE, Campion DS, Bohan A, Harris R, Levy J, *et al.* Muscle disease in progressive systemic sclerosis: diagnostic and therapeutic considerations. *Arthritis Rheum* 1978;**21**:62–71.
20 **Della Rossa A**, Valentini G, Bombardieri S, Bencivelli W, Silman AJ, D'Angelo S, *et al.* European multicentre study to define disease activity criteria for systemic sclerosis. I. Clinical and epidemiological features of 290 patients from 19 centres. *Ann Rheum Dis* 2001;**60**:585–91.
21 **Steen VD**. Scleroderma renal crisis. *Rheum Dis Clin North Am* 1996;**22**:861–78.
22 **Roberts NK**, Cabeen WR, Moss J, Clements PJ, Furst DE. The prevalence of conduction defects and cardiac arrhythmias in progressive systemic sclerosis. *Ann Intern Med* 1981;**94**:38–40.
23 **Nagasako T**, Sugiyama T, Mizushima T, Miura Y, Kato M, Asaka M. Up-regulated Smad5 mediates apoptosis of gastric epithelial cells induced by Helicobacter pylori infection. *J Biol Chem* 2003;**278**:4821–5.
24 **Contin C**, Pitard V, Itai T, Nagata S, Moreau JF, Dechanet-Merville J. Membrane-anchored CD40 is processed by the tumour necrosis factor-α-converting enzyme. *J Biol Chem* 2003;**278**:32801–9.
25 **Atamas SP**, White B. The role of chemokines in the pathogenesis of scleroderma. *Curr Opin Rheumatol* 2003;**15**:772–7.
26 **LeRoy EC**, Mercurio S, Sherer GK. Replication and phenotypic expression of control and scleroderma human fibroblasts: responses to growth factors. *Proc Natl Acad Sci USA* 1982;**79**:1286–90.
27 **Prescott RJ**, Freemont AJ, Jones CJP, Hoyland J, Fielding P. Sequential dermal microvascular and perivascular changes in the development of scleroderma. *J Pathol* 1992;**166**:255–63.
28 **Kräling BM**, Maul GG, Jimenez SA. Mononuclear cellular infiltrates in clinically involved skin from patients with systemic sclerosis of recent onset predominantly consist of monocytes/macrophages. *Pathobiology* 1995;**63**:48–56.
29 **Tamby MC**, Chanseaud Y, Guillevin L, Mouthon L. New insights into the pathogenesis of systemic sclerosis. *Autoimmun Rev* 2003;**2**:152–7.
30 **Galindo M**, Santiago B, Rivero M, Rullas J, Alcami J, Pablos JL. Chemokine expression by systemic sclerosis fibroblasts: abnormal regulation of monocyte chemoattractant protein 1 expression. *Arthritis Rheum* 2001;**44**:1382–6.
31 **Bolster MB**, Ludwicka A, Sutherland SE, Strange C, Silver RM. Cytokine concentrations in bronchoalveolar lavage fluid of patients with systemic sclerosis. *Arthritis Rheum* 1997;**40**:743–51.
32 **Anderegg U**, Saalbach A, Haustein UF. Chemokine release from activated human dermal microvascular endothelial cells—implications for the pathophysiology of scleroderma? *Arch Dermatol Res* 2000;**292**:341–7.
33 **Minty A**, Chalon P, Guillemot JC, Kaghad M, Liauzun P, Magazin M, *et al.* Molecular cloning of the MCP-3 chemokine gene and regulation of its expression. *Eur Cytokine Netw* 1993;**4**:99–110.
34 **Ong VH**, Evans LA, Shiwen X, Fisher IB, Rajkumar V, Abraham DJ, *et al.* Monocyte chemoattractant protein 3 as a mediator of fibrosis. Over expression in systemic sclerosis and type 1 tight-skin mouse. *Arthritis Rheum* 2003;**48**:1979–91.
35 **Schmuth M**, Neyer S, Rainer C, Grassegger A, Fritsch P, Romani N, *et al.* Expression of the C-C chemokine MIP-3α/CCL20 in human epidermis with impaired permeability barrier function. *Exp Dermatol* 2002;**11**:135–42.
36 **Black RA**, Rauch CT, Kozlosky CJ, Peschon JJ, Slack JL, Wolfson MF, *et al.* A metalloproteinase disintegrin that releases tumour-necrosis factor-α from cells. *Nature* 1997;**385**:729–33.
37 **Moss ML**, Jin SLC, Milla ME, Burkhart W, Carter HL, Chen WJ, *et al.* Cloning of a disintegrin metalloproteinase that processes precursor tumour-necrosis factor-α. *Nature* 1997;**385**:733–6.
38 **Ohta S**, Harigai M, Tanaka M, Kawaguchi Y, Sugiura T, Takagi K, *et al.* Tumour necrosis factor-α (TNF-α) converting enzyme contributes to production of TNF-α in synovial tissues from patients with rheumatoid arthritis. *J Rheumatol* 2001;**28**:1756–63.
39 **Patel IR**, Attur MG, Patel RN, Stuchin SA, Abagyan RA, Abramson SB, *et al.* TNF-α convertase enzyme from human arthritis-affected cartilage: isolation of cDNA by differential display, expression of the active enzyme, and regulation of TNF-α. *J Immunol* 1998;**160**:4570–9.
40 **Seifert T**, Kieseier BC, Ropele S, Strasser-Fuchs S, Quehenberger F, Fazekas F, *et al.* TACE mRNA expression in peripheral mononuclear cells precedes new lesions on MRI in multiple sclerosis. *Mult Scler* 2002;**8**:447–51.
41 **Mezyk R**, Bzowska M, Bereta J. Structure and functions of tumour necrosis factor-α converting enzyme. *Acta Biochim Pol* 2003;**50**:625–45.
42 **Ermert M**, Pantazis C, Duncker HD, Grimminger F, Seeger W, Ermert L. In situ localization of TNF-α/β, TACE and TNF-receptors TNF-R1 and TNF-R2 in control and LPS-treated lung tissue. *Cytokine* 2003;**22**:89–100.
43 **Allavena P**, Piemonti L, Longoni D, Bernasconi S, Stoppacciaro A, Ruco L, *et al.* IL-10 prevents the differentiation of monocytes to dendritic cells but promotes their maturation to macrophages. *Eur J Immunol* 1998;**28**:359–69.
44 **Mizui Y**, Yamazaki K, Sagane K, Tanaka I. cDNA cloning of mouse tumour necrosis factor-α converting enzyme (TACE) and partial analysis of its promoter. *Gene* 1999;**233**:67–74.
45 **Holmes A**, Abraham DJ, Sa S, Shi-wen X, Black CM, Leask A. CTGF and SMADS, maintenance of scleroderma phenotype is independent of SMAD signalling. *J Biol Chem* 2001;**276**:10594–691.
46 **Gruschwitz MS**, Vieth G. Up-regulation of class II major histocompatibility complex and intracellular adhesion molecule 1 expression on scleroderma fibroblasts and endothelial cells by interferon-γ and tumour necrosis factor α in the early disease stage. *Arthritis Rheum* 1997;**40**:540–50.
47 **Gruschwitz MS**, Albrecht M, Vieth G, Haustein U. In situ expression and serum levels of tumour necrosis factor-α receptors in patients with early stage of systemic sclerosis. *J Rheumatol* 1997;**24**:1936–43.
48 **Ellman M**, MacDonald PA. Etanercept as treatment for diffuse scleroderma: a pilot study [abstract]. *Arthritis Rheum* 2000;**43**(suppl 9):S392.
49 **Grell M**, Douni E, Wajant H, Löhden M, Clauss M, Maxeiner B, *et al.* The transmembrane form of tumour necrosis factor is the prime activating ligand of the 80 kDa tumour necrosis factor receptor. *Cell* 1995;**83**:793–802.
50 **Tartaglia LA**, Pennica D, Goeddel DV. Ligand passing: the 75-kDa tumour necrosis factor (TNF-) receptor recruits TNF- for signalling by the 55-kDa TNF-receptor. *J Biol Chem* 1993;**268**:18542–8.
51 **Grell M**, Wajant H, Zimmermann G, Scheurich P. The type 1 receptor (CD120a) is the high-affinity receptor for soluble tumour necrosis factor. *Proc Natl Acad Sci USA* 1998;**95**:570–5.
52 **Malinin NL**, Boldin MP, Kovalenko AV, Wallach D. MAP3K-related kinase involved in NF-κB induction by TNF, CD95 and IL-1. *Nature* 1997;**385**:540–4.
53 **Pimentel-Muinos FX**, Seed B. Regulated commitment of TNF-receptor signalling: a molecular switch for death or activation. *Immunity* 1999;**11**:783–93.
54 **Peschon JJ**, Slack JL, Reddy P, Stocking KL, Sunnarborg SW, Lee DC, *et al.* An essential role for ectodomain shedding in mammalian development. *Science* 1998;**282**:1281–4.
55 **Abraham DJ**, Shiwen X, Black CM, Sa S, Xu Y, Leask A. Tumour necrosis factor α suppresses the induction of connective tissue growth factor by transforming growth factor-β in normal and scleroderma fibroblasts. *J Biol Chem* 2000;**275**:15220–5.
56 **Yamane K**, Ihn H, Asano Y, Jinnin M, Tamaki K. Antagonistic effects of TNF-α on TGF-β signalling through down-regulation of TGF-β receptor type II in human dermal fibroblasts. *J Immunol* 2003;**171**:3855–62.
57 **Conway JG**, Andrews RC, Beaudet B, Bickett DM, Boncek V, Brodie TA, *et al.* Inhibition of tumour necrosis factor-α (TNF-α) production and arthritis in the rat by GW3333, a dual inhibitor of TNF-α-converting enzyme and matrix metalloproteinases. *J Pharmacol Exp Ther* 2001;**298**:900–8.

ARTHRITIS & RHEUMATISM
Vol. 52, No. 9, September 2005, pp 2697–2707
DOI 10.1002/art.21258

Butyrate Suppresses Tumor Necrosis Factor α Production by Regulating Specific Messenger RNA Degradation Mediated Through a *cis*-Acting AU-Rich Element

Jun Fukae, Yoshiharu Amasaki, Yumi Yamashita, Toshiyuki Bohgaki, Shinsuke Yasuda, Satoshi Jodo, Tatsuya Atsumi, and Takao Koike

Objective. **To study the capacity of butyrate to inhibit production of tumor necrosis factor α (TNFα) in macrophage-like synoviocytes (MLS) from patients with rheumatoid arthritis (RA), in human peripheral monocytes, and in murine RAW264.7 macrophages.**

Methods. **The concentrations of TNFα in culture supernatants of these cells were measured using enzyme-linked immunosorbent assay. The expression levels of various messenger RNAs (mRNA), such as those for TNFα, the mRNA-binding protein TIS11B, and luciferase, were measured using real-time quantitative polymerase chain reaction. The in vitro effects of butyrate on transcriptional regulation were evaluated by transfection with various reporter plasmids in RAW264.7 macrophages. The effects of TIS11B on TNFα expression were examined using an overexpression model of TIS11B in RAW264.7 cells.**

Results. **Butyrate suppressed TNFα protein and mRNA production in MLS and monocytes, but paradoxically enhanced transactivation of the TNFα promoter. Expression of the AU-rich element (ARE)–binding protein TIS11B was up-regulated by butyrate. Induction of TNFα mRNA by lipopolysaccharide was significantly inhibited when TIS11B was overexpressed. Butyrate facilitated the degradation of luciferase transcripts containing the 3′-untranslated region (3′-UTR) of TNFα, and this effect was dependent on the ARE in the 3′-UTR that is known to be involved in the regulation of mRNA degradation.**

Conclusion. **These results indicate that butyrate suppresses TNFα expression by facilitating mRNA degradation mediated through a *cis*-acting ARE. Butyrate has the ability to regulate TNFα at the mRNA level and is therefore a potential therapeutic drug for RA patients.**

Rheumatoid arthritis (RA) is a chronic inflammatory disease characterized by cartilage destruction and extracellular matrix degradation in multiple joints (1). The pathogenesis of RA is not clearly understood; however, tumor necrosis factor α (TNFα) is involved in its development, a conclusion which is supported by successful treatments with anti-TNFα reagents (2). The production of TNFα was found to be increased in rheumatoid synovium, followed by the induction of other proinflammatory cytokines, including interleukin-1β (IL-1β), IL-6, and IL-8, as well as matrix metalloproteinases involved in cartilage and bone destruction in RA (3–5). These cytokines are involved in synovial cell activation and proliferation, leading to generation of pannus (6).

Synovial tissue consists of heterogeneous immune and non–immune cell populations, including fibroblast-like synoviocytes, macrophage-like synoviocytes (MLS), lymphocytes, dendritic cells, and endothelial cells (7). Among these populations, MLS originating from bone marrow–derived monocytes are largely responsible, upon activation, for the production of TNFα protein (6). Monocytes can give rise to osteoclasts involved in rheumatoid bone destruction (8). The mech-

Supported by the Ministry of Education, Science, Technology, Sports, and Culture of Japan (grant 14570004) and by a research grant for study of the action of short chain fatty acids on cytokine gene regulation.

Jun Fukae, MD, PhD, Yoshiharu Amasaki, MD, PhD, Yumi Yamashita, PhD, Toshiyuki Bohgaki, MD, PhD, Shinsuke Yasuda, MD, PhD, Satoshi Jodo, MD, PhD, Tatsuya Atsumi, MD, PhD, Takao Koike, MD, PhD: Hokkaido University Graduate School of Medicine, Sapporo, Japan.

Address correspondence and reprint requests to Yoshiharu Amasaki, MD, Department of Medicine II, Hokkaido University Graduate School of Medicine, Kita-15, Nishi-7, Kita-ku, Sapporo 060-8638, Japan. E-mail: yamasaki@med.hokudai.ac.jp.

Submitted for publication December 6, 2004; accepted in revised form June 3, 2005.

anisms of MLS activation have been only partially understood. Macrophages express TNFα via activation of Toll-like receptor 4–NF-κB signaling, and this type of activation may be mimicked experimentally by administration of lipopolysaccharide (LPS) (9,10).

TNFα-mediated chronic inflammation has also been studied in inflammatory bowel diseases and in animal models of such diseases. In those studies, physiologic roles for short-chain fatty acids have been identified (11,12). Short-chain fatty acids are a natural product of colonic anaerobic fermentation of dietary fiber by luminal microflora. These are the preferred sources of energy for the normal colonic epithelial cell, and they can modulate a variety of fundamental cellular processes to induce cell-cycle arrest, differentiation, and apoptosis in transformed cells (13,14). These molecules, especially butyrate, have potent antiinflammatory effects and can modulate TNFα expression in colonic epithelial cells and in monocytes (15). It has also been shown that administration of butyrate suppresses experimental enteritis induced in mice by dextran sulfate sodium (16). Experiments in colonocytes revealed that butyrate down-regulates TNFα expression by modulating NF-κB–DNA binding activity (15), although the precise mechanism is not fully understood. In addition, butyrate is known to function as a histone deacetylase (HDA) inhibitor in cells, and it can induce alteration of the chromatin structure (17,18), although the effect of this activity on TNFα down-regulation is not yet understood. We investigated whether butyrate could suppress TNFα production in activated synovial cells and macrophages, in order to evaluate short-chain fatty acids as a potential investigational new treatment for chronic inflammation in RA.

MATERIALS AND METHODS

Preparation of primary synoviocytes and culture. Primary synoviocytes were obtained from surgically resected synovial tissue from Japanese patients with RA. Informed consent was obtained from each patient. Tissue specimens were minced and dissociated in Hanks' balanced salt solution (Invitrogen, Carlsbad, CA) containing 5 mg/ml type I collagenase (Sigma, St. Louis, MO) and 0.15 mg/ml DNase I (Sigma) for 2 hours at 37°C. Samples were then passed through a metal mesh and a nylon mesh, each with a 100-μm pore size. Cells were collected by centrifugation and resuspended at 0.5×10^6/ml in Iscove's modified Dulbecco's medium (Invitrogen) containing 10% heat-inactivated fetal bovine serum (FBS) and antibiotics. The resulting synoviocytes were cultured in a 6-well tissue culture plate (Becton Dickinson, Mountain View, CA) at 37°C in a humidified atmosphere with 5% CO_2 for 24–48 hours. Our primarily rheumatoid synoviocyte cultures contained ~10–35% of a CD14-positive subpopulation as assessed by fluorescence-activated cell sorting (FACS Calibur system; Becton Dickinson) (data not shown). The proportion of CD14-positive rheumatoid synoviocytes varied depending on the patient's background, such as duration or activity of the disease and treatment. Before the stimulation assay, nonadherent cells were removed by washing twice with phosphate buffered saline (PBS).

Cell culture and stimulation. Human monocytes were enriched from whole blood obtained from healthy Japanese volunteers. The mononuclear cell fraction was prepared by density-gradient centrifugation over Ficoll-Paque (Amersham Biosciences, Uppsala, Sweden), followed by plating in culture medium at 37°C for 1 hour in a humidified incubator to obtain the adherent cells. After washing the cells twice with PBS, adherent cells were resuspended in RPMI 1640 medium (Invitrogen) containing 10% heat-inactivated FBS and antibiotics, then counted and diluted to 0.5×10^6/ml. Cells were processed for the stimulation assay on the same day that the blood was collected. Purity of CD14-positive cells was 80–90% as assessed by fluorescence-activated cell sorting (data not shown). The murine macrophage cell line RAW264.7 (no. TIB-71; American Type Culture Collection, Rockville, MD) was grown in Dulbecco's modified Eagle's medium (DMEM; Invitrogen) containing 10% heat-inactivated FBS and antibiotics at 37°C in a humidified atmosphere with 5% CO_2 (19). Cells were resuspended at 0.25×10^6/ml, then 2 ml/well of the cell suspension was transferred to 6-well tissue culture plates, followed by 24 hours of culture before stimulation. After preincubation, cells were stimulated with LPS (no. L4391; Sigma) or were used without stimulation. In some experiments, various concentrations of sodium butyrate (Sigma) were included in the culture. Where indicated, actinomycin D (Sigma) was also included in the culture to restrict transcriptional events.

RNA preparation and real-time quantitative polymerase chain reaction (PCR) analysis. Total RNA was obtained by using TRIzol RNA Reagent (Invitrogen) according to the manufacturer's instructions. In some experiments, total RNA was extracted from transfected cells using the Concert Cytoplasmic RNA Reagent (Invitrogen) in combination with DNase I Amplification Grade (Invitrogen) to eliminate residual plasmid DNA. RNA samples were reverse-transcribed using oligo(dT) primers and ReverTra Ace (Toyobo, Osaka, Japan) according to the manufacturer's instructions. Real-time quantitative PCR analyses were performed using 100 n*M* TaqMan probe and 200 n*M* forward and reverse primers in a final volume of 30 μl using 2×PCR reagent (Applied Biosystems, Chiba, Japan) in an ABI PRISM 7000 Sequence Detection System instrument (Applied Biosystems) based on dual-labeled fluorogenic probe technology (20).

The following forward and reverse primers and TaqMan probes, designed by Primer Express software (Applied Biosystems), were used for analyses: mouse TNFα, forward primer 5′-CAGACCCTCACACTCAGATCATCT-3′, reverse primer 5′-GCACCACTAGTTGGTTGTCTTTGA-3′, TaqMan probe 5′-CAAGCCTGTAGCCCACGTCGTAGCA-3′; mouse TIS11B, forward primer 5′-TTGTTGGTAGCTTCTGGCTTGA-3′, reverse primer 5′-GGCATCTACTGACAAAAGATGGAA-3′, TaqMan probe 5′-TCCATTTCATAGCCCACTTAACCACGCA-3′; luciferase, forward primer 5′-TGACCGCCTGAAGTCTCTGA-3′, reverse primer 5′-

ACACCTGCGTCGAAGATGTTG-3′, TaqMan probe 5′-CCGCTGAATTGGAATCCATCTTGCTC-3′; AU-rich element (ARE) mutation, forward primer 5′-ATGCACAG-CCTTCCTCACAG-3′, reverse primer 5′-CCCGGCCT-TCCAAATAAATAC-3′, minor groove binder (MGB) TaqMan probe 5′-TATCCATTATCCATCCATTATCCATC-3′. The first 3 TaqMan probes were labeled on the 5′ end with FAM reporter dye and on the 3′ end with TAMRA quencher dye; the ARE mutation MGB TaqMan probe was labeled on the 5′ end with FAM reporter dye and on the 3′ end with conjugated MGB.

To measure the gene copy number of the various transcripts, the purified artificial gene product containing an amplification sequence was serially diluted to achieve a standard curve. Data for each messenger RNA (mRNA) quantity were normalized based on the mRNA copy number of GAPDH obtained using the TaqMan rodent GAPDH control reagents (Applied Biosystems).

Enzyme-linked immunosorbent assay (ELISA). The concentrations of human and mouse TNFα proteins were determined using specific sandwich ELISA kits (no. 656227 from Cosmo Bio [Tokyo, Japan] and no. 10019 from Genzyme [Cambridge, MA], respectively) according to the manufacturers' instructions.

Plasmid construction. The luciferase reporter plasmids pNFκB-Luc and pGL3-BASIC were purchased from Stratagene (La Jolla, CA) and Promega (Madison, WI), respectively. Murine genomic DNA extracted from a normal C57BL/6 mouse using a standard protocol (21) was used for amplification of a genomic DNA fragment of the mouse TNFα gene. A 0.9-kb DNA fragment corresponding to the 5′-untranslated region (5′-UTR) of the mouse TNFα gene was PCR-amplified with the sense and antisense primers 5′-CTC-AAGCTTATCAGAGTGAAAGGAGAAGGC-3′ and 5′-CTCAAGCTTAGTGAAAGGGACAGAACCTGC-3′, respectively. The product was inserted into the *Hind* III cloning site of pGL3-BASIC and designated pGL-mTNFα. The 0.8-kb 3′-UTR of the mouse TNFα gene was similarly amplified using PCR, and the *Xba* I and *Bam* HI restriction sites were introduced with the PCR primers 5′-TCTAGAGGGAATGGG-TGTTCATCC-3′ and 5′-GGATCCCATGCCCCAGGGCAAA-3′, respectively. The resulting DNA fragment was used to replace the 3′-UTR of the pGL-mTNFα, and the resulting plasmid was designated pGL-mTNFα-UTR.

A pGL-CMV-UTR plasmid, in which the luciferase gene was constitutively expressed under the control of the cytomegalovirus (CMV) promoter, was generated by replacing the *Hind* III fragment corresponding to the TNFα promoter region in the pGL-mTNFα-UTR vector with a DNA fragment containing the CMV promoter sequences from pFLAG-CMV-2 (Sigma). In addition, the AT repeat (ARE) in pGL-CMV-UTR corresponding to the TNFα 3′-UTR sequence (+1299 to +1332) was mutated to yield an ARE mutation plasmid (pGL-CMV-UTR/mARE) using standard recombinant techniques and the mutagenic oligonucleotide 5′-ACAGCCTTCCTCACAGAGCCAGCCCCCCTCTATT-TATATTTGCACTTATTATCCATTATCCATCCATTAT-CCATCCATTTGCTTATGAATGTATTTATTTGGAAG-GCCG-3′. The sequences of all the DNA fragments obtained by PCR amplification were confirmed by DNA sequencing and completely matched the reported mouse TNFα genomic sequence (GenBank accession no. Y00467) (22).

A mammalian expression plasmid, pFLAG-TIS11B, that encodes mouse TIS11B complementary DNA (cDNA) (23) was generated by introducing a mouse full-length TIS11B cDNA fragment into the pFLAG-CMV-2 plasmid (Sigma). The TIS11B cDNA fragment was obtained by PCR amplification of cDNA from RAW264.7 cells and the specific sense and antisense primers 5′-GAATTCGATGACCACCACCCTCGT-3′ and 5′-TCTAGAGGAGAGGTGAAGGAGGCATG-3′, respectively. After subcloning into pCR-blunt and confirmation by DNA sequencing, the 1.2-kb fragment corresponding to the TIS11B cDNA (GenBank accession no. BC016621) was excised and ligated into pFLAG-CMV-2 at the *Xba* I and *Eco* RI cloning sites.

Transfection and luciferase assay. RAW264.7 cells (0.25×10^5) were transferred to 8-cm tissue culture plates (Becton Dickinson) and incubated for 24 hours to 70% confluence. Transfections were achieved using Transfectam reagent (Promega), according to the manufacturer's instructions, with the plasmids described above. Plasmid DNA (10 μg) was mixed with 20 μl of Transfectam reagent in 3 ml of FBS-free DMEM and transferred to the plates. After 2 hours of incubation, complete culture medium was added to the cells, followed by further incubation to semiconfluence. The transfection efficiency in the current protocol was ~5% when cells transfected with green fluorescent protein–expressing plasmid were analyzed by fluorescence-activated cell sorting (data not shown). Transfected cells were collected and distributed into new 6-well tissue culture plates (Becton Dickinson) before the stimulation assay. This step was performed to equalize the number of transfected cells and eliminate any differences in transfection efficiency between plates.

Where indicated, the luciferase assay was carried out according to the procedure described previously with minimal modifications (24). Briefly, RAW264.7 cells were transfected with various reporter plasmids as described above. After incubation and stimulation, cells were lysed using lysis buffer (Promega). Cell lysates were stored at −80°C until the luciferase assay was performed. The protein content of each sample was determined using a protein assay reagent (Bio-Rad, Hercules, CA), and the luciferase activities of the samples were normalized according to the protein content of the samples. Data are reported as relative luciferase units.

Cell proliferation assay. In order to exclude the possibility that butyrate directly affects cell viability, a proliferation assay was performed using MTS (3-(4,5-dimethylthiazol-2-yl)-5-(3-carboxymethoxyphenyl)-2-(4-sulfophenyl)-2H-tetrazolium) tetrazolium assay (Cell Titer96 AQueous One Solution Cell Proliferation Assay; Promega). RAW264.7 cells (0.25×10^5) were transferred into microtiter-plate wells in 100 μl of DMEM containing various concentrations of butyrate, then MTS reagent was added to the wells. Optical density was read using a microplate autoreader (Microplate Reader Model 3550; Bio-Rad) at a wavelength of 490 nm after addition of MTS reagent.

Statistical analysis. Statistical analyses were calculated by Student's *t*-test with the use of the Excel program (Microsoft, Redmond, WA).

RESULTS

Suppression by butyrate of TNFα protein production in cultured primary synoviocytes. We first analyzed the effect of butyrate on TNFα production in rheumatoid synoviocytes during stimulation with LPS. When primary synoviocytes were stimulated with LPS, significant amounts of TNFα protein were detected in the culture supernatants (Figure 1A). Addition of butyrate to the culture medium led to a significant, dose-dependent decrease in LPS-stimulated TNFα production. MLS, major producers of TNFα in the rheumatoid inflammatory synovium, play an important role in the initiation of synovitis and bone destruction (25). We paid attention to the subpopulation of monocyte/macrophages, and thus we repeated the experiments on the effect of butyrate on TNFα production both by peripheral monocytes and by the macrophage cell line RAW264.7. Human peripheral monocytes and RAW264.7 cells both secreted significant amounts of TNFα upon LPS stimulation (Figures 1B and C). As was the case in the primary cell culture, there was a significant decrease in LPS-stimulated TNFα secretion with increasing butyrate concentrations in the medium. In all experiments, similar GAPDH mRNA expression levels were confirmed in each cell preparation after treatment with LPS/butyrate (data not shown).

RAW264.7 cells were exposed to various concentrations of butyrate, and MTS tetrazolium assay was performed to assess cell proliferation. The results revealed that butyrate had no significant effect on cell proliferation (Figure 2B).

Suppression by butyrate of TNFα expression at the mRNA level in monocytes and in the macrophage cell line RAW264.7. To determine how butyrate regulates TNFα production in monocytes, we next examined the effect of butyrate on TNFα mRNA expression. We performed semiquantitative reverse transcriptase (RT)–PCR analysis using specific primers for initial screening and found that butyrate suppressed TNFα mRNA induction in response to stimulation with LPS in human monocytes (data not shown). Butyrate also suppressed LPS-stimulated TNFα production in RAW264.7 cells in a dose-dependent manner, confirmed by real-time quantitative PCR (Figure 2A). The macrophage cell line RAW264.7 is responsive to butyrate; therefore, we used the RAW264.7 cells as an appropriate system for transfection assay.

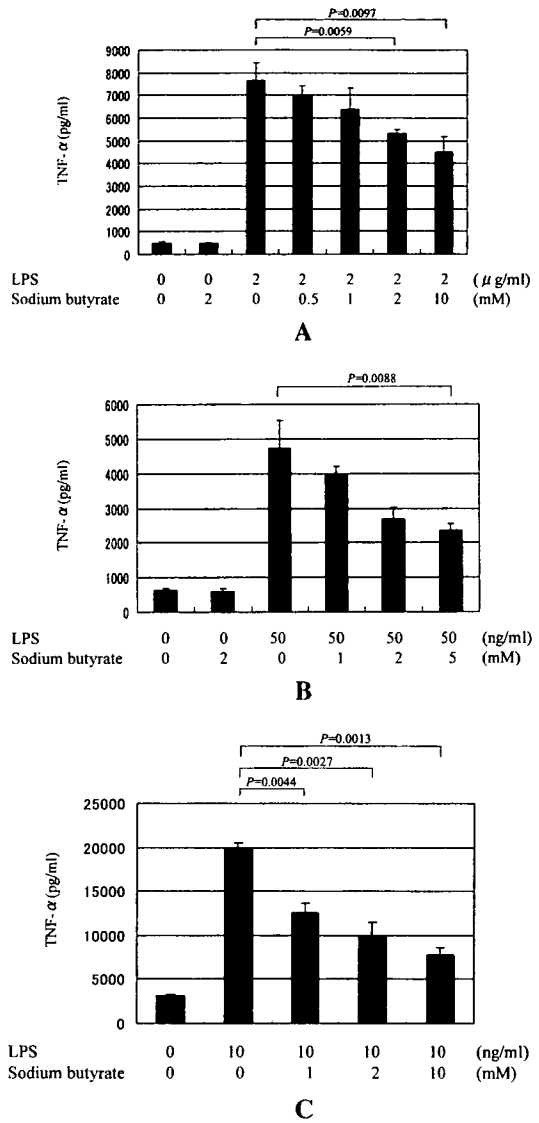

Figure 1. Effects of butyrate on tumor necrosis factor α (TNFα) protein secretion by synoviocytes and monocytes. An enzyme-linked immunosorbent assay (ELISA) specific for human TNFα protein was used to determine levels of TNFα in **A,** culture supernatants of primary synoviocytes (obtained from patients with rheumatoid arthritis) not stimulated with lipopolysaccharide (LPS) or stimulated with 2 μg/ml LPS for 6 hours in the presence or absence of sodium butyrate, and **B,** human peripheral blood monocytes (obtained from healthy donors) not stimulated with LPS or stimulated with 50 ng/ml LPS for 4 hours in the presence or absence of sodium butyrate. **C,** Levels of mouse TNFα were measured in culture supernatants from RAW264.7 cells not stimulated with LPS or stimulated with 10 ng/ml LPS for 6 hours in the presence or absence of sodium butyrate, using an ELISA specific for mouse TNFα. Experiments in **A, B,** and **C** were repeated 15, 9, and 6 independent times, respectively, and representative results are shown. Values are the mean and SEM.

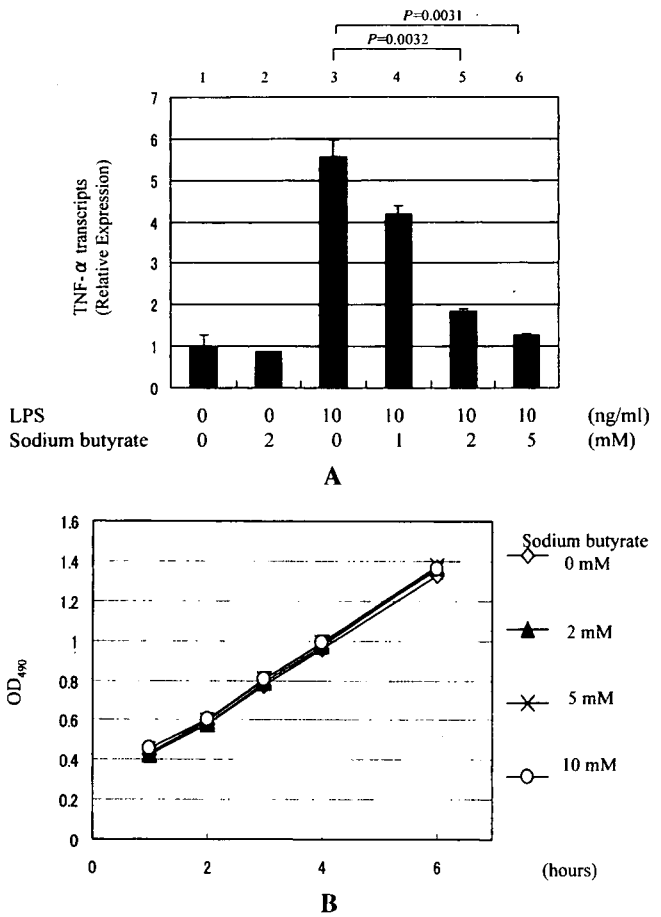

Figure 2. Effects of butyrate on TNFα mRNA expression and cell proliferation in RAW264.7 cells. **A,** Real-time quantitative polymerase chain reaction (PCR) (described in Materials and Methods) was used to estimate TNFα expression in RAW264.7 cells not stimulated with LPS (lanes 1 and 2) or stimulated with 10 ng/ml LPS (lanes 3–6) in the presence (lanes 2 and 4–6) or absence (lanes 1 and 3) of sodium butyrate for 2 hours. The amount of TNFα cDNA transcripts is displayed as a relative value obtained by dividing the value for TNFα transcripts by the value for GAPDH cDNA transcripts. Real-time quantitative PCR data were obtained from triplicate transwells and are representative of 3 independent experiments. Values are the mean and SEM. **B,** Cell proliferation assay (described in Materials and Methods) was used to examine the toxicity of butyrate on RAW264.7 cells. Cells were treated with various concentrations of butyrate (0, 2, 5, and 10 m*M*), and the optical density (OD) was read at a wavelength of 490 nm serially at 1-, 2-, 3-, 4-, and 6-hour time points. Data were obtained from triplicate transwells. Values are the mean ± SEM of 3 independent experiments. See Figure 1 for other definitions.

No suppression by butyrate of transcriptional activity driven through the TNFα promoter. To test whether butyrate could affect TNFα mRNA expression via transcriptional repression, RAW264.7 cells were transfected with reporter plasmids containing the consensus NF-κB binding sequence or the full-length TNFα promoter sequence. When cells were transfected with pNFκB-Luc or pGL-mTNFα, however, butyrate did not suppress the transcriptional activities (Figures 3A and B). Instead, butyrate showed a dose-dependent enhancement of transactivation, which was inconsistent with its effects on the mRNA and protein expression of TNFα. These results indicate that butyrate regulates TNFα mRNA levels via a mechanism other than transcriptional repression in RAW264.7 cells.

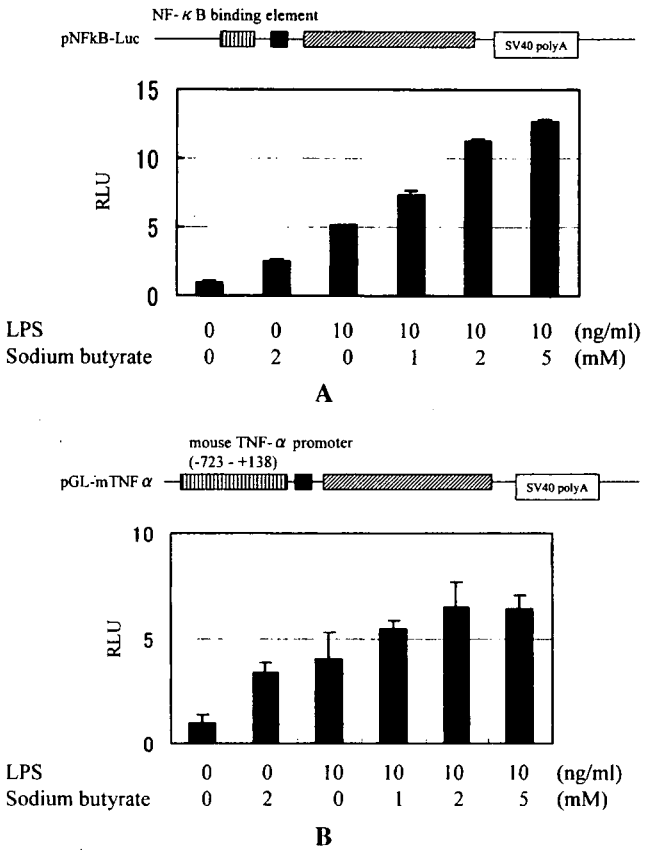

Figure 3. Effect of butyrate on TNFα promoter–related transcriptional activities. RAW264.7 cells were transfected with various types of luciferase reporter plasmids (see Materials and Methods for description of methods of transfection and luciferase assay). Forty-eight hours after transfection, cells were stimulated with 10 ng/ml LPS in the absence or presence of sodium butyrate (1, 2, or 5 m*M*) for 6 hours. The luciferase activities in cell lysates were measured and normalized using the protein concentration in each sample. **A,** Transcriptional activity of cells transfected with pNFκB-Luc. **B,** Transcriptional activity of cells transfected with pGL-mTNFα. Data shown in **A** and **B** were obtained from triplicate transwells and are representative of 6 independent experiments. Values are the mean and SEM. SV40 polyA = simian virus 40 late poly(A) signal; RLU = relative luciferase units (see Figure 1 for other definitions).

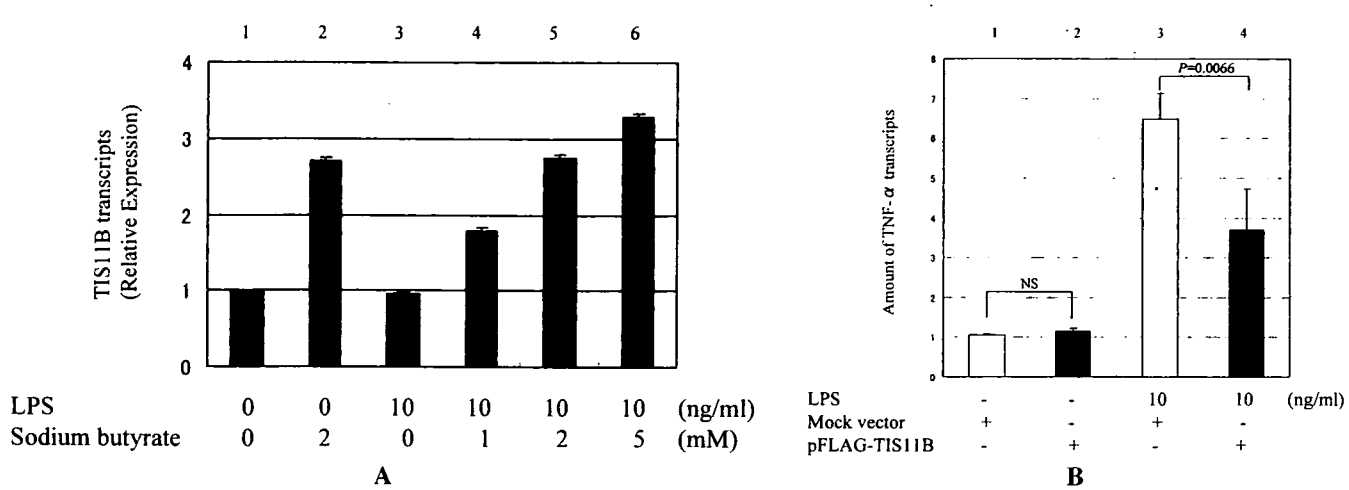

Figure 4. Expression of the tristetraprolin (TTP) family of genes in RAW264.7 cells upon treatment with butyrate. **A,** Expression of mRNA for TIS11B (a representative member of the TTP family of proteins) in RAW264.7 cells upon treatment with butyrate. RAW264.7 cells were not stimulated with LPS or were stimulated with 10 ng/ml LPS (lanes 3–6) in the presence (lanes 2 and 4–6) or absence (lanes 1 and 3) of butyrate. After 1 hour of stimulation, total RNA was obtained, followed by real-time quantitative polymerase chain reaction (PCR) for TIS11B. The amount of TIS11B cDNA transcripts is displayed as a relative value obtained by dividing the value for TIS11B transcripts by the value for GAPDH cDNA transcripts. Real-time quantitative PCR data were obtained from triplicate transwells and are representative of 3 independent experiments. Values are the mean and SEM. **B,** Effect of TIS11B on expression levels of TNFα mRNA in RAW264.7 cells stimulated with LPS. RAW264.7 cells were transfected with the TIS11B expression vector, pFLAG-TIS11B (solid bars) or with the control pFLAG empty (mock) vector (open bars). Forty-eight hours after transfection, cells were stimulated with 10 ng/ml LPS (lanes 3 and 4); total RNA was obtained after 2 hours of stimulation. The amount of TNFα cDNA transcripts was determined using real-time quantitative PCR. Data are schematically displayed as a relative value obtained by dividing the value for TNFα transcripts by the value for GAPDH cDNA transcripts. Real-time quantitative PCR data were obtained from triplicate transwells and are representative of 3 independent experiments. Values are the mean and SEM. NS = not significant (see Figure 1 for other definitions).

TIS11B as a candidate molecule for butyrate-mediated inhibition of TNFα mRNA expression. TNFα gene expression involves posttranscriptional regulation, including the ARE in the 3′-UTR that is thought to play a critical role in the regulatory mechanism (26). AREs are found in multiple cytokine genes including TNFα, and the *cis*-regulatory effects of these elements are mediated by several polypeptides that can bind AREs. Tristetraprolin (TTP) is an ARE-binding protein that facilitates TNFα mRNA degradation, and TIS11B and TIS11D are representative members of the TTP family of proteins that are also capable of interacting with AREs. We hypothesized that the effects of butyrate were related to the posttranscriptional regulation mediated through the AREs and ARE-binding proteins. To search for the butyrate-mediated induction of ARE-binding proteins, we first used semiquantitative RT-PCR to screen for the expression of TTP family proteins such as TTP, TIS11B, and TIS11D in RAW264.7 cells treated with butyrate. Among the factors examined, butyrate induced only TIS11B mRNA but neither TTP mRNA nor TIS11D mRNA (data not shown). Real-time quantitative PCR revealed that butyrate induced TIS11B mRNA in a dose-dependent manner (Figure 4A).

We determined that TIS11B had a suppressive effect on levels of TNFα mRNA. RAW264.7 cells were transfected with TIS11B expression plasmid or with a control mock vector, then stimulated with LPS. The expression level of TNFα mRNA decreased significantly in RAW264.7 cells transfected with TIS11B expression plasmid (Figure 4B). These results suggested that butyrate down-regulated levels of TNFα mRNA via binding of TIS11B to an ARE.

Facilitation by butyrate of mRNA degradation via the function of an ARE in the TNFα 3′-UTR. We next studied whether the inhibitory effects of butyrate on TNFα specifically depended on an ARE. To determine whether butyrate affects the amounts of gene transcripts carrying the TNFα 3′-UTR, we designed a real-time TaqMan RT-PCR–based quantitative assay that detects mRNA turnover (Figure 5). RAW264.7 cells were transfected with pGL-CMV-UTR reporter plasmid and treated with actinomycin D to repress generation of newly transcribed mRNA. To equalize the difference in transfection efficiency between plates, all transfected

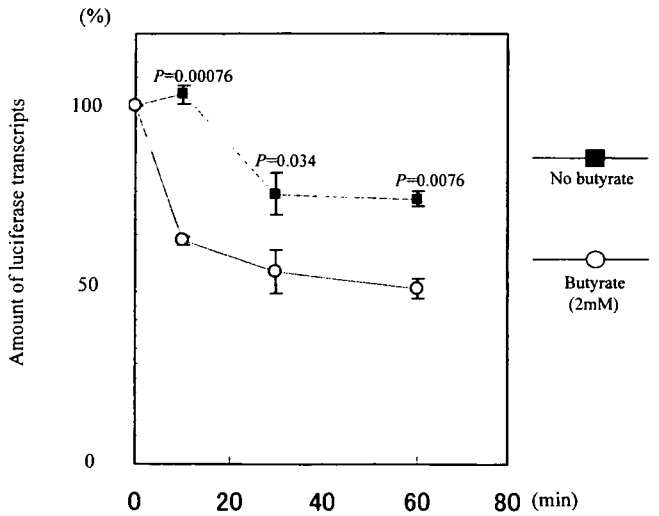

Figure 5. Effect of butyrate on the turnover of luciferase mRNA containing a tumor necrosis factor α 3′-untranslated region. RAW264.7 cells were transfected with pGL-CMV-UTR (see Materials and Methods). After no treatment or pretreatment with butyrate (2 m*M*) for 2 hours, cells were placed in culture medium containing actinomycin D (10 μg/ml) to halt transcription. Cells were then harvested serially at 0-, 10-, 30-, and 60-minute time points, and total RNA was extracted. After extensive treatment with RNase-free DNase I to digest the plasmid vector DNA, total RNA samples were reverse-transcribed for real-time quantitative polymerase chain reaction using primers specific for the luciferase gene product (described in Materials and Methods). The amount of luciferase cDNA transcripts is displayed as a relative value obtained by dividing the value for luciferase transcripts by the value for GAPDH cDNA transcripts. The datum at the 0-minute time point (for luciferase/GAPDH) was assigned a value of 100%, and other data are shown relative to this value. Values are the mean ± SEM of 3 independent experiments.

cells were collected and distributed into new plates before butyrate treatment. The time course of decrease of mRNA levels was in direct proportion to the rate of degradation. The amount of cDNA transcripts containing the 3′-UTR was serially quantified by real-time PCR. We observed a significant decrease in cDNA transcripts derived from pGL-CMV-UTR in cells treated with butyrate, both at the 10-minute time point and thereafter (Figure 5). This suggested that butyrate facilitated the degradation of mRNA transcripts of TNFα carrying the 3′-UTR sequence.

In various cytokine genes, including TNFα, an ARE in the 3′-UTR has been shown to affect stability of the gene transcripts (26). To test whether the inhibitory effects of butyrate on TNFα are mediated by the action of this *cis* ARE, we generated pGL-CMV-UTR/mARE containing a mutated ARE from pGL-CMV-UTR (Figure 6A). The amounts of transcripts derived from these plasmids were quantified and compared using RAW264.7 cells and the TaqMan PCR method. In this assay, total amounts of transcripts derived from mixed plasmids were determined by reactions using a luciferase TaqMan probe, and, at the same time, amounts of transcripts carrying the ARE mutation derived from these mixed plasmids were determined using an ARE mutation MGB TaqMan probe (Figure 6A). The quantification of these 2 transcripts was made possible by using a common gene standard, R-luc-AU, that contained both the mutated ARE and part of the common luciferase open reading frame sequence, and changes in the expression of these 2 transcripts were described as a ratio and calculated as follows: transcripts with mutated ARE:transcripts with intact ARE = (M/G):([A − M]/G) = M:(A − M), where A is the total amount of luciferase transcripts, M is the amount of transcripts with mutated ARE, and G is the internal control GAPDH.

As shown in Figure 6B, the amount of transcripts carrying mutated ARE and the amount carrying intact ARE were almost identical at the time point at which actinomycin D had stopped the transcription, when cells were treated (or not treated) with butyrate. It was shown that the relative amount of transcripts carrying a mutated ARE increased significantly during the time course. Thus, transcripts carrying the mutated ARE were more stable than those carrying intact ARE, and butyrate's ability to facilitate the degradation of transcripts was lost when the ARE was mutated. This indicates that the suppressive effect of butyrate on TNFα expression is mediated through the specific ARE in the 3′-UTR of the TNFα transcript.

DISCUSSION

In this report, we have shown that butyrate strongly down-regulated the production of TNFα in primary synoviocytes, peripheral monocytes, and murine RAW264.7 macrophages at the mRNA level. Our results also indicated that butyrate induced an ARE-binding protein, TIS11B, that could facilitate TNFα mRNA degradation. The collective data led us to believe that the down-regulation of TNFα expression by butyrate was mediated through the TIS11B protein that bound to a specific ARE and facilitated mRNA degradation.

TNFα is a key cytokine in the pathogenesis of RA. Therefore, inhibition of the action of TNFα may improve the clinical course of patients with RA. Biologic agents designed to interfere with the action of TNFα

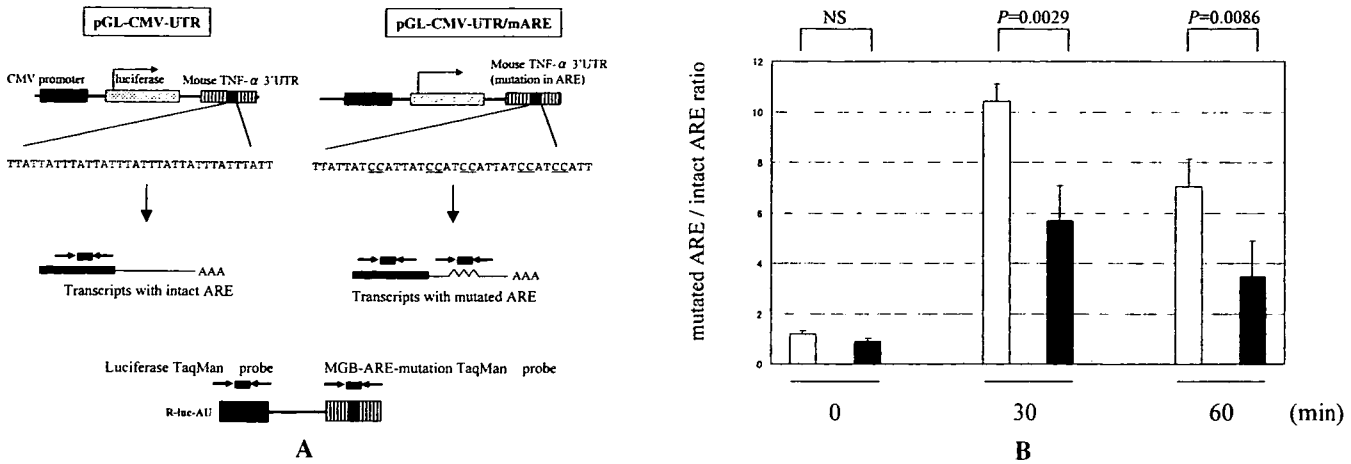

Figure 6. Effects of mutations in AU-rich elements (AREs) on the ability of butyrate to modify mRNA turnover. **A,** Schematic diagram of the plasmids, primers, and TaqMan probes that were used in these experiments. The plasmid pGL-CMV-UTR/mARE was derived by mutating the ARE of the 3′-untranslated region (3′-UTR) of the plasmid pGL-CMV-UTR (see Materials and Methods). To measure the gene copy number of the transcripts derived from pGL-CMV-UTR and pGL-CMV-UTR/mARE, the artificial DNA fragment R-luc-AU was generated from pGL-CMV-UTR/mARE by polymerase chain reaction (PCR) amplification. The R-luc-AU fragment, which contained both the ARE mutation and part of the common luciferase open reading frame sequence, was used to produce both the standard curve for the total luciferase transcripts and the curve for transcripts containing the ARE mutation. **B,** Quantitative PCR analysis of the reporter gene products carrying intact or mutated ARE. RAW264.7 cells were transfected with a 50:50 mixture of pGL-CMV-UTR/mARE and pGL-CMV-UTR. Cells were then not treated (solid bars) or pretreated with 5 m*M* sodium butyrate for 2 hours (open bars) and placed in culture medium containing actinomycin D (10 μg/ml) to halt transcription. Cells were then harvested serially at 0-, 30-, and 60-minute time points, and total RNA was extracted. Degradation of plasmid DNA and subsequent cDNA synthesis were carried out using the same method described in Figure 5. Real-time quantitative PCR analyses were done using a TaqMan probe, with specific forward and reverse primers (see Materials and Methods). The amounts of total luciferase cDNA transcripts and transcripts with mutated ARE were determined, and the y-axis shows the ratio of cDNA transcripts with mutated ARE to cDNA transcripts with intact ARE. Data were obtained from triplicate transwells and are representative of 5 independent experiments. Values are the mean and SEM. CMV = cytomegalovirus; TNFα = tumor necrosis factor α; MGB = minor groove binder; NS = not significant.

have been approved for the treatment of RA, and they provide dramatic efficacy for the affected patients. However, the disadvantages of biologic agents, such as their high cost, their instability, the difficulty of producing them, and the immune reaction of the host toward them, remain to be addressed. Therefore, new chemical agents that down-regulate TNFα production have been researched extensively. Our current findings may provide a framework for the therapeutic down-regulation of TNFα production by butyrate or its analogs.

Butyrate facilitated the degradation of luciferase transcripts when the TNFα 3′-UTR cDNA sequence was included in the reporter construct. This effect appeared to be dependent on an ARE, since a mutation in the ARE in the reporter plasmids resulted in the loss of the butyrate-induced changes in the transcript turnover. Thus, butyrate could down-regulate TNFα mRNA expression by facilitating TNFα mRNA degradation through a mechanism that was dependent on the specific ARE.

AREs are several repetitive sequences of AUUUA or UUAUUUAUU present in the 3′-UTRs of various mRNA. The AREs are clustered into several categories and have been identified in a panel of genes other than TNFα (27–30). These genes largely encode proteins that regulate cellular growth and the body's response to exogenous agents such as microbes and inflammatory and environmental stimuli. The mRNA containing AREs are commonly short lived, rapidly expressed in response to stimuli, and rapidly degraded once their critical role in gene regulation ceases.

To date, several ARE-binding proteins have been reported that can stabilize or destabilize the target mRNA by binding competitively to their AREs. TTP (also known as TIS11, Nup475, and G0S24) is one of these ARE-binding proteins, and it has been characterized as a critical factor that controls TNFα mRNA turnover (31). Interestingly, genetically manipulated mice that lack TTP showed an abundance of endogenous TNFα production, an RA-like arthritis, and autoimmunity, presumably mediated by an excess of TNFα (32–34). TTP-related proteins, designated TIS11B and TIS11D, are structurally similar to TTP in their zinc-finger motifs, and they share functions with TTP, al-